SAPIENZA
Università di Roma
Facoltà di Farmacia e Medicina

Dottorato di Ricerca in
MORFOGENESI e INGEGNERIA TISSUTALE

XXXI Ciclo
(A.A. 2017/2018)

Identification and characterization of the role of CALR protein and 3'untranslated region in normal and neoplastic hematopoiesis

Dottorando
Alberto Quattrocchi

Tutor
Prof. Clara Nervi

Coordinatore
Prof. Antonio Musarò

CONFIDENTIALITY NOTICE

Reviewers and PhD committee members are obliged to keep the files confidential and to delete all records after completing the review process.

Il ricevimento degli elaborati scientifici, per l'ottenimento del titolo di Dottore di Ricerca, in qualità di Membro del Collegio dei Docenti del Dottorato in Morfogenesi ed Ingegneria Tissutale richiede di osservare le seguenti normative:

i. considerare le Informazioni confidenziali e riservate come strettamente private e ad adottare tutte le ragionevoli misure finalizzate a mantenerle tali;

ii. utilizzare le Informazioni confidenziali e riservate unicamente allo scopo per le quali sono state fornite o rese note, impegnandosi a non divulgarle a soggetti terzi le informazioni contenute negli elaborati ricevuti;

iii. a garantire la massima riservatezza, anche in osservanza alla vigente normativa in materia di marchi, di copyright e di brevetti per invenzioni industriali e in base alla normativa sulla privacy, ai sensi del D.Lgs. 196/2003, riguardo il know-how e tutte le informazioni acquisite, che non potranno in alcun modo, in alcun caso e per alcuna ragione essere utilizzate a proprio o altrui profitto e/o essere divulgate e/o riprodotte o comunque rese note a soggetti terzi.

INDEX

The thesis explained

Myeloproliferative Neoplasms (MPNs) are hematopoietic stem cell-derived clonal disorders including polycythemia vera (PV), essential thrombocythemia (ET) and primary myelofibrosis (PMF), with an overproduction of red blood cells, platelets and bone marrow fibrotic tissue, respectively. MPNs are triggered by JAK2, MPL and CALR (CALR) somatic mutations, all deregulating JAK/STAT signalling. CALR mutations, which are exclusively associated to ET and PMF, generally arise from a +1 frameshift converting the first 31 nucleotides of CALR-3'UTR, into coding sequence. However, the physiologic role of CALR and such CALR-3'UTR region in hematopoiesis are unknown.
This thesis was aimed to: i) investigate the role of CALR in physiological hematopoiesis and the context of MPN; ii) elucidate the function of novel mutated variants of CALR 3'UTR that we identified; iii) realize a model *in vitro* to study the functional consequences of CALR 3'UTR disruption in myelopoiesis.
Results and conclusions. We observed a hematopoietic lineage-specific regulation of CALR. Moreover, in a cohort of MPN patients, we detected two non-canonical CALR mutations associated to enhanced erythropoiesis in patients diagnosed as JAK2V617F-negative PVs. One was an in frame mutation (c.1214_1225del/del12), whereas the other occurred in the 3'UTR (c.1254+10_+33del/del24). Interestingly, the RNA folding prediction of del24, and even more of del12 indicated a structural impairment of this 3'UTR region. Primary CD34+ cells from such patients exhibited an erythroid growth push on unilineage culture and colony assays, associated with JAK/STAT activation and increase of CALR expression. Strikingly, CALR 3'UTR disruption in myeloid progenitors by CRISPR-CAS9 technology increased CALR levels and JAK/STAT activation, and, more surprisingly, induced erythropoiesis. Overall, these results suggest a novel role for CALR-3'UTR in lineage fate decision of myeloid progenitors. Its disruption might induce a PV-phenotype *in vitro* and *in vivo*.

1. Introduction

1.1 Hematopoiesis: focus on myelopoiesis.

The entire demand of whole blood cells during individuals' lifespan comes from a finely regulated process named as hematopoiesis. It consists of an intricate pattern of molecular, cellular and phenotypic changes that originates cells with different fates and lineages and which is orchestrated by external cues, such cytokines signaling, and internal cues, a wide set of transcription factors, long non coding RNA (lncRNA) and microRNAs (miRNA)[1].

The study of hematopoiesis over decades relied on the combination of different techniques that established the actual knowledge about hematopoietic differentiation tree. The support of mouse as experimental model frequently preceded the homologous discovery in human. First approaches entailed morphological observations of bone marrow and peripheral blood cells. Histological stains and electron microscopy allowed identifying distinct profiles at different stages of maturation[2]. Nevertheless, if morphological analysis is useful to point out peculiarities of lineage-specific cell morphology at the later stages of differentiation, this technique is not much informative about early stages. In this sense further insights were reached by progenitors transplantation in lethally irradiated mice and measuring the repopulation of blood elements and the formation of spleen colonies, which is still considered a measure of stem cells regenerative potential. Later the development of *in vitro* colony assays allowed additional identification of early progenitors even for human, especially for myeloid series, classifying cell populations based on functional capability of generating colonies of distinct lineages[3-5]. Flow-cytometry analysis subsequently added new possibilities of classifying and characterizing single differentiation steps with monoclonal antibodies, introducing several surface markers panels. Recent advances of omics studies for proteomic, transcriptomic and epigenomic rewired the classical picture of hematopoiesis,

which it is now enriched of heterogeneity, despite keeping its original backbone[6].

Within the microenvironment of bone marrow, Hematopoietic Stem Cells (HSCs) are the pool of cells that sustain the entire human hematopoiesis. As stem cells, HSCs hold two basic properties, multipotency, the capability of generate multiple subtypes of cells by asymmetric division, and self-renewal, the maintenance of a reserve pool through replicating itself. Basing on these properties, HSCs can be distinguished in two types of cells, long-term-HSC (lt-HSC) and short-term-HSC (st-HSC). Lt-HSCs ($LIN^-/IL\text{-}7R\alpha^-/CD34^-/SCA1^+/KIT^+/FLT3^-/Thy1^{low}$) retain all differentiation potential and self-renewal, and are responsible for the hematopoietic reservoir during individuals lifespan[7]; st-HSCs ($LIN^-/IL\text{-}7R\alpha^-/CD34^+/SCA1^+/KIT^+/FLT3^{low}/Thy1^{low}$) derive from lt-HSC and retain the same potential, but have reduced self-renewal since they are committed to initiate the differentiation process[8].

First differentiation events entail the genesis of multipotent progenitors (MPPs) from HSCs, extensively described in mice by a combination of cell markers that reveal a heterogeneous class of different progenitors (MPP1, MPP2, MPP3, MPP4)[9]. Lt-HSC, st-HCS and MPP are slightly different degrees of self-renewal loss, measured by a progressively reduced capacity of persistence in mice recipients after transplantation[10, 11].

Later along differentiation but historically earlier identified by flow cytometry, the two fundamental branches of hematopoiesis arise from these progenitors, the common myeloid progenitor (CMP, $LIN^-/SCA1^-/KIT^+/CD34^+/Fc\gamma RII^-/Fc\gamma RIII^-$) generating erythrocytes, megakaryocytes, granulocytes and monocytes[12], and the common lymphoid progenitor (CLP, $LIN^-/IL\text{-}7R\alpha^+/SCA1^{low}/KIT/^{low}$), originating lymphocytes B, T and Natural Killer (NK)[13]. These two differentiation programs are known as myelopoiesis and lymphopoiesis respectively.

Myelopoiesis is the differentiation process from which erythrocytes (E), megakaryocytes (Mk), granulocytes (G), and monocytes (M) arise through a sequence of commitment events.
Further lineage specification define how terminally differentiated cells are generated. Two main fate choices develop the remaining part of myelopoiesis tree, although this vision recently has been challenged. According to classical heamatopoiesis, from CMP two committed progenitors take origin, the Megakaryocytes/ Erythrocytes progenitor (MEP) and Granulocytes/Monocytes progenitor (GMP).
Myeloid routes of differentiation following CMP were variously characterized by in vitro colony assay. Each committed progenitor for erythroid, megakaryocyte, monocyte and macrophage has an in vitro assayed counter part known as Burst Forming Unit (BFU) and Colony Forming Unit (CFU). Typically BFU are intended as earlier progenitors than CFU, and in the assay give rise to a higher number of cells within the colony (exactly a "burst") respect to CFU[14, 15]. Only erythroid BFU-E producing hemoglobin (BFU-E) and megakaryocytic BFU-E (BFU-Mk) have been observed in colony assays, whereas for all myeloid lineages CFU-E, CFU-Mk, CFU-G and CFU-M are widely described[16]. The importance of such assays lies in the opportunity of identifying specific progenitor populations, otherwise morphologically indistinguishable, relying on their functional behavior. This functional identification has been further accompanied by cytofluorimetric analysis, for instance highlighting how BFU-E and CFU-E are $CD45^{+}$ cells, with a transition from the first to the latter denoted by the increase of transferrin receptor (from $CD71^{low}$ to $CD71^{high}$); moreover BFU-E proliferation is dependent by stem cell factor and erythropoietin (EPO), whereas CFU-E growth depend exclusively by EPO[17].
In the last phase of differentiation, myeloid maturation is identifiable by means of optical microscopy. Indeed terminal stages of myelopoiesis entail clearly recognizable morphologies in the bone marrow, since the resolution of each lineage is marked by

cytological and histological modification, observable by appropriate staining. Along the megakaryocyte fate, the committed progenitor CFU-Mk develops in megakaryoblast. Under stimulus of thrombopoietin (TPO) megakaryoblast starts to replicate nucleus without completing cell division, from 8 to 64 nuclei, finally generating the mature megakaryocyte, from which platelets arise. Granulopoiesis is the branch differentiation that produces granulocytes, (eosinophils basophils, neutrophils), through specific stages of myeloblast, promyelocyte, myelocyte, metamyelocite and band cell. Monocytes complete their differentiation from monoblast and promonocyte; when becomes active, monocyte migrates from blood flow to tissue, terminally maturating as macrophage.
In the erythroid lineage, the first morphologically identifiable committed progenitor arising from CFU-E is pro-erythroblast (pro-E). Pro-E is featured by a large nucleus, with some nucleolus, and free ribosomes that make the cytoplasm partially basophilic. From pro-erythroblast erythroblasts differentiates, encompassing the stages of basophilic erythroblast, polychromatic erythroblast and orthochromatic erythroblast. Basophylic erythroblast is smaller with more marked basophilia than pro-erythroblast, due to the increase in protein synthesis accomplished by higher number of polyribosomes. Afterwards, at the stage of polychromatophylic erythroblast, the hemoglobin synthesis increase leads to the compensation of such basophilia with acidophilia, resulting in a heterogeneous stain of cytoplasm, whence these cells are named polychromatophylic. Within the nucleus, that reduces its dimension, a more heterochromatinic state is observed. In the subsequent stage of orthochromatophylic erythroblast the nucleus is strongly condensed, with prominent eosinophilia of cytoplasm, due to the additional increase of hemoglobin. The terminal phases includes the expulsion of nucleus, forming the reticulocytes, with a mild basophilia due to the still high number of polyribosomes; reticulocytes are ready to pass from bone marrow to the bloodstream, finally producing erythrocytes[2] (fig. 1.1).

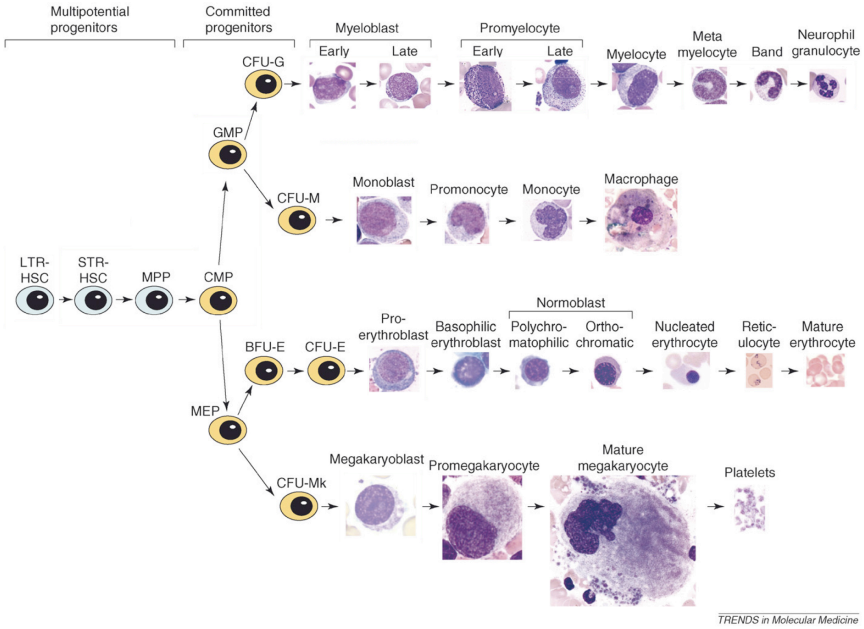

Figure 1.1. Diagram of differentiation stages in myelopoiesis. Schematic representation of commitment events from LTR-HSC towards the myeloid progenitors and terminal differentiated cells. Morphology of each differentiating stage is showed. Adapted from Krause DS et al., *Trends Mol Med*, 2007[18].

Cluster differentiation further identified these transitions; pro-E shows high levels of CD71 and the stemness marker CD117; during the differentiation towards erythroblasts, CD117 is lost, keeping high levels of CD71 with the appearance of CD235a. Terminal differentiation to erythrocytes entails the further increase of CD235a, with dropping of CD71[19].

Underlying morphologies and markers, several molecular mechanisms are at the base of myelopoiesis. Myeloid committed progenitors are driven towards terminal maturation even by extrinsic factors. Cytokines, a wide class of signal molecules produced by specialized cells, transduce proliferation and differentiation cues within cells by means of specific receptors. Erythropoietin (EPO) is the key-signal required by erythroid

differentiation, Thrombopoietin (TPO) pushes Mk progenitors towards platelets maturation, whereas granulocyte colony stimulation factor (GCSF) is required for granulocytic differentiation. All these cytokines are bound by specific receptors, such as erythropoietin receptor (EPOR), MPL proto-oncogene, thrombopoietin receptor (TPOR/MPL), granulocyte colony stimulating factor receptor (GCSFR), all associated with tyrosine-kinase Janus kinase 2 (JAK2). Cytokine-receptor interaction induces receptor dimerization and JAK2 auto-phosphorylation, leading to STATs transcription factors phosphorylation. Thus such signaling promotes a gene expression response determining proliferation, differentiation and survival[20]. Furthermore, extrinsic cues act on internal stimuli. Indeed key events in the stepwise process of myelopoiesis are the expression or repression of transcription factors that are mutually exclusive in determining cell fate, since the activation of a set implies the repression of another one. At early stages, key transcription factors of myeloid differentiation are relatively limited, such PU.1, CAAT enhancer binding protein (CEBPα and CEBPβ), NFIA, TAL1, GATA1, LMO2. The fine-tuning of their transcriptional regulation in turn, often with contribute of miRNAs outputs the sum of these multiple stimuli, generating the proper lineage differentiation as a result of a complex circuital regulation[21].

Finally, due to single-cell data analysis, the rigid and hierarchical model of hematopoiesis has been recently challenged. Albeit defined steps of fate choice from HSC to MPPs and myeloid and lymphoid progenitors are considered still valid relatively to the cell surface markers, RNA-seq data on single cells are indicating an extremely heterogeneous population among HSCs and progenitors, and it is becoming more evident that the assumption of a specific differentiation program and the progressive loss of self renewal are not strictly connected. These recent insight suggest that probably HCSs are committed towards one or more lineages of differentiation at very early stages; moreover, different progenitors might share the same differentiation output, and they possibly

maintain replicative potential also in advanced stages of hematopoiesis[6].

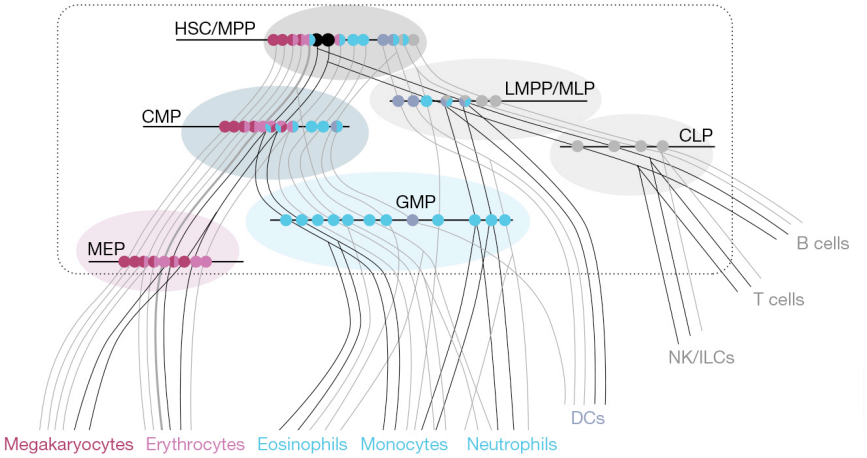

Figure 1.2. Revised representation of hematopoieis. According to recent single cell analysis, hierarchical model of hematopoietic differentiation have been revised, proposing a trajectory model where HSC compartment is indeed a heterogeneous population (represented by different colours). Historical categories of progenitors are indeed group of various committed cells, some times bi- or tri-lineage, as indicated by multicolours. From Laurenti E et al., *Nature, 2018*[6].

1.2. Myeloproliferative Neoplasms.

When the natural course of hematopoiesis is disrupted and the delicate balance of blood cells production is deregulated, a complex class of pathologies named as Leukemia arises. Leukemia is a condition of malignancy that implies an uncontrolled accumulation of leukocytes. When affecting the myeloid lineage, it could be distinct in Acute Myeloid Leukemia (AML) and Chronic Myeloid Leukemia (CML) according to the undifferentiated or differentiated status of cells, respectively. Besides these kinds of malignancy, another pre-malignant condition perturbing the myeloid lineage are Myeloproliferative Neoplasms (MPNs). In MPNs the abnormal proliferation of myeloid progenitors causes an overproduction of one terminally differentiated cell population and

affects the homeostasis of the bone marrow. MPNs are distincted from CML by the absence of Philadelphia Chromosome translocation, which in the past had been largely used as cytogenetic marker for differential classification[18].

1.2.1 Clinics and classification

Myeloproliferative Neoplasms (MPNs) develops when clonal hematopoiesis leads to mature blood myeloid cells overproduction, with complete differentiation. Clonal expansion of these cells affects primarily the HSCs and a single clone acquires proliferative advantage over the HSCs population. Three phenotypes, partially overlapping, are observed within this group of pathologies. Polycythemia Vera (PV) leads to the accumulation of erythrocytes, Essential Thrombocythemia (ET) is associated to the overproduction of platelets, whereas Primary Myelofibrosis (PMF), the most adverse form, progressively leads to reticular fibrosis of bone marrow.

Aberrant JAK/STAT signaling, which is a guide force of myeloid maturation, combined with a variety of factors such age, genetic background and sex, determines the peculiar phenotype of each MPN. The progression of disease is another factor that increase the heterogeneity of these pathologies, since both PV and ET might evolve in PMF, and all could lead to acute myeloid leukemia in a small percentage of cases (1.5%, 7% and 11% for ET, PV and PMF respectively)[22]. From this point of view studying the mechanisms at the base of MPNs might give the unique opportunity to understand an extremely precocious phase of cancer onset, commonly precluded to observation in most of overt tumors.

1.2.2 Driver Mutations

The insurgence of sporadic mutations was the first molecular property identified for MPNs, after years of exclusively clinic diagnosis. Such mutations are named as driver because they are thought to be responsible for proliferative advantage of the HSC clone. Clonal hematopoiesis could be identified by the amount of

cells bearing such mutations, albeit other factors such age and sex are required to observe the onset. Main driver mutations affect JAK2, MPL, a truncated form of the thrombopoietin receptor, and CALR (CALR) genes.
$JAK2^{V617F}$, a single nucleotide substitution, was the first driver mutation identified and the most frequent across MPNs. Later other mutations affecting JAK2 exon 12 were identified. MPL mutations are more various. In all cases, JAK2 and MPL mutations are activating respect to the physiological signaling of JAK/STAT, constitutively triggering it. In this sense CALR mutations identification was unexpected, since functionally distant from myelopoiesis, by contrast with JAK2 and MPL. The most frequent mutated gene in MPN is JAK2 (97% in PV, 55% in ET and 50% in PMF). CALR and MPL seem to be exclusive of ET and PMF with a frequency of 36/30% and 4/8%, respectively. However, driver mutations do not furnish an exhaustive clarification of molecular mechanisms that cause MPNs, as indirectly proven by a considerable fraction of patients without any of such alterations, together with the observation that driver mutations could be detected already in young individuals, even if they do not present any MPN clinical symptom. Nowadays, therapy is substantially palliative and several progresses in the comprehension of MPNs etiology are required. Therefore, the identification of still unknown myeloid actors, potentially impaired in MPNs, might contribute to the ultimate advocated progress in diagnosis and therapy.

1.3. Calreticulin (CALR)

CALR is a multifunctional protein of 46 kDa, resident mainly, but not exclusively, in the endoplasmic reticulum (ER). Its most commonly known functions are calcium buffering within the ER and chaperone, assisting the folding of newly synthetized proteins.

1.3.1 Structure and Domains

The primary structure of CALR from N-terminal to C-terminal consists of an N-domain, a P-domain and a C-domain (fig. 1.2).

The N-domain, presenting the ER-localization signal peptide, has been reported to bind alfa-integrin subunit; the P-domain presents two stretch series of proline repetitions, which generate a lectine-like structure; lastly the C-domain is responsible for the regulation of calcium buffering. The C-terminal extreme tail of CALR presents the amminoacidic sequence Lysine-Aspartate-Glutammate-Leucin (KDEL), which is specifically recognized by the ER KDEL-receptor and thereby ensures the retrieval of CALR in the ER lumen, avoiding that CALR as well as others ER resident protein accidentally follows the secretory pathway; however, some experimental evidences challenge the paradigm of an exclusively ER-protein, as explained below.

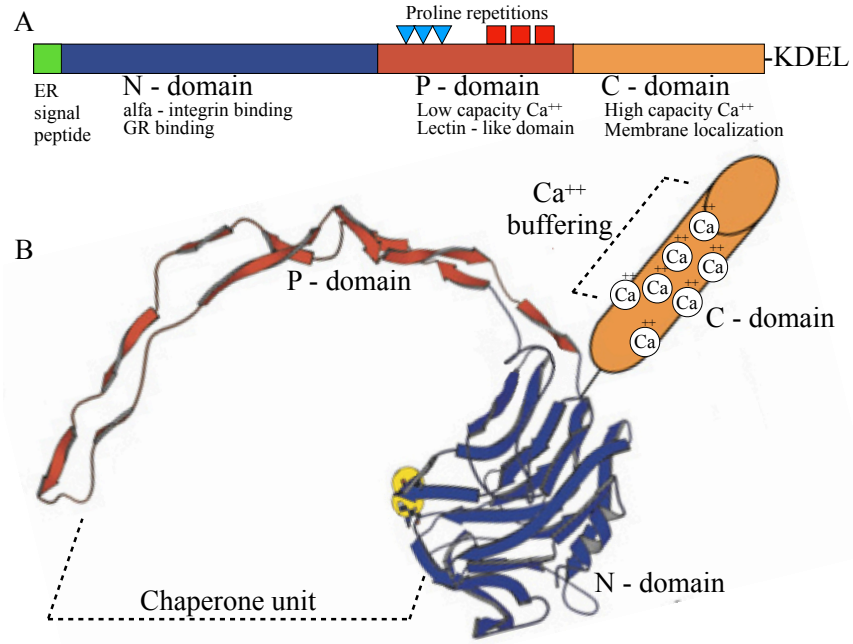

Figure 1.3. Primary sequence, domains and 3D structure model of CALR. (A) Scheme of main CALR domains. GR, Glucocorticoid Receptor. ER localization signal and N, P and C domain are shown in green, blue, red and orange respectively. (B) Graphical model of CALR structure, with the same colours legend of (A). Functional domains structures are indicated. Adapted from Michalak M, *Biochem J.*, 2009[23].

1.3.2 ER Functions.

CALR has been originally described in the context of ER, where the main functions are strictly related to its structural domains: chaperone and Calcium (Ca^{++}) binding. The lectin-like domain, located within the N-domain and recognizing various residues of carbohydrates, ensures the interaction with other ER chaperones, mostly Protein Disulfide Isomerase (PDI) and Endoplasmic Reticulum Protein 57 (ErP57), thereby regulating their chaperone activities. In turn, these interactions are tightly dependent from the other core feature of CALR, which is Calcium (Ca^{++}) binding. The chaperon function is actually linked to the lectin domain in cooperation with P-domain, involving CALR in the folding quality control of glycosylated protein. This activity is accomplished in association with Calnexin, a highly similar transmembrane-ER chaperone. All glycosylated protein reach the ER lumen labeled by a N-oligosaccharide, composed by 2 residues of N – acetylglucosamine, 9 residues of mannose, and 3 residues of glucose ($Glc_3Man_9GlcNAc_2$). 2/3 of glucose residues are removed by specific glucosidases, generating $Glc_1Man_9GlcNAc_2$, recognized by the chaperone system of Calnexin and CALR. Such interaction blocks the nascent protein within the ER, allowing its proper folding assisted by CALR; trough repetitive cycles of addition and removal of glucose, the protein is retained in ER until reaching the correct structure and is addressed to the secretory pathway, otherwise is destined to proteasome degradation[24].

The other classically known function of CALR, partially connected with the chaperon function, is Ca^{++} binding, regulating its free moiety in the ER lumen, and within cytoplasm.

It has been reported that over 50% of ER Ca^{++} is bound by CALR[23]. CALR presents two site of Calcium binding respectively in P-domain and C-domain. The calcium binding at P-domain is at high affinity (KD=1 μM) but low capacity (1 mol Ca^{++}/1 mol CALR), whereas C-domain calcium binding has low affinity (KD=1 mM) but high capacity (25 mol Ca^{++}/1 mol CALR)[23]. The

considerable amount of Ca^{++} that CALR is capable to bind makes this protein an important candidate as master regulator of Ca^{++} dependent pathways. Indeed, it has been proposed that own CALR might regulate the Ca^{++} concentration within the ER lumen ($[Ca^{++}]_{ER}$), since overexpression and knockdown models of CALR alters the ER Ca^{++} stores[25, 26]. Moreover the formation of complexes between CALR and other chaperones are regulated by $[Ca^{++}]_{ER}$ that affects the amount of Ca^{++} bound by CALR[27]. In the end, modifying $[Ca^{++}]$ structural changes of CALR conformation have been observed[28]. Importantly, Ca^{++} signalling might operate downstream EPOR pathway, during erythropoiesis[29].
It should be mentioned that the complexity of CALR functions might be reconsidered according a recently highlighted property of such protein. Indeed, CALR is considered an intrinsically-disordered protein, a class of proteins that present a high structural instability, both restricted to specific domains and extended to the whole protein. More properly, CALR is a mixed composition of different regions, with a high degree of disorder and structure instability at the P and the end of C domain, whereas N-domain and the N-terminal half of C-domain are more globular[30].
Beyond chaperone and calcium buffering, CALR is reported in several cell processes that considerably differ each other, challenging the definition of "ER-resident protein".

1.3.3 Extra-ER functions

One of the most characterized extra-ER functions is related to apoptosis. It has been showed that CALR localizes at the membrane surface of various cells and interacts with LDL-related-receptor-protein (LRP), exposed on the macrophage membrane. The interaction CALR-LRP conveys within macrophage a signal inducing phagocytosis. If the same cell on its membrane contextually expresses CD47, and the latter binds the ligand SIRPalpha on macrophage surface, an anti-apoptotic signal is transduced within macrophage, and the pro-apoptotic signaling of CALR is surmounted. When CD47-SIRPalpha interaction is

disrupted, the complex CALR-LRP manage to activate phagocytosis[31]. Moreover, it has been recently showed that CALR membrane localization for apoptosis signaling is dependent by phosphatidylserine-binding through the C-terminal domain of CALR[32].

CALR is described interacting with several partners of different nature. Evidence of CALR in vitro binding to the peptide sequence KLGFFKR[33], highly similar to cytoplasm domain of alfa-integrin, was followed by proofs of involvement in cell adhesion[34]. The same domain is present on glucocorticoid receptor (GR), a widely known nuclear factor, guiding to identify as well a GR binding activity by CALR[35]. From this demonstrated interaction, a controversial debate arises about the involvement of CALR in modulating gene expression within nucleus. An early paper demonstrated a nuclear localization of CALR, thereby hypothesizing some nuclear activity[36]; later these findings were considered to be artifacts[37]. After recent works demonstrating a nuclear export activity of CALR on GR[38], the latest theory proposes that the apparent nuclear localization has to be intended just as perinuclear proximity, due to the localization in the ER region that faces nucleus. In this sense the GR nuclear export mediated by CALR has been recently described in the context of stress erythropoiesis, showing that CALR represses GR activity by removing it from nucleus and resetting the stress response; this activity is impaired in $JAK2^{V617F}$ PV patients, where GR are constitutively active because JAK/STAT signaling might compromise CALR nuclear export activity[39].

It deserves to be mentioned that some papers report an RNA binding activity of CALR in disparate biological scenarios. The first evidence, in simian, refers to the recognition by CALR of GC reach structures on RNA^{+} strand of Rubella Virus[40]. Later Timchenko et al., followed by other works, described a repressive interaction between CALR and the 5'UTR mRNA of C/EBPα, resulting in an impairment of C/EBPα translation in vitro[41, 42], and in samples from AML patients[43]. Recently this repression has been

observed as a result of unfolded protein response (UPR) in AML patients[44], suggesting that extra-ER CALR might act as key actor of myelopoiesis, unexpectedly not yet investigated in MPNs.
All such experimental proofs assume a basic property of CALR, rarely studied but essential to accept the accomplishment of such tasks: CALR should have some mechanisms to escape the ER. This question was addressed by a work conducted in various cell lines, where the authors applied a specific assay to measure the localizing properties of each single CALR domain conjugated with PDI, used as ER-lumen report protein. As expected, N-domain keeps the ER-localization, P-domain has no influence, but surprisingly C-domain can induce the "retrotranslocation" of PDI from ER to cytosol[45]. Although restricted to C-domain and possibly missing the effects driven by the complete interaction pattern of full length CALR, such data further remarks the functional dynamicity of this protein.

1.3.4 Recurrent mutations of CALR and known role in MPNs.
In such intricate context of multiple functions, the identification of CALR mutants associated to ET and PMF in 2013, resulted unexpected because any previous evidence of a hematopoietic function for this protein was missing. The most common CALR mutations identified in MPNs were a 52 bp deletion (c.1099_1150del52 - L367fs*46) and a 5 bp insertion (c.1154_1155insTTGTC - K385fs*47), routinely named as type 1 and type 2, respectively. Besides these two most frequent variants, there is a wide continuous of heterogeneous deletions, insertions and complex insertion/deletion (indel). However, independently from the specific mutation considered, CALR coding sequence varies always in a unique fashion. In fact type 1, 2 and all others less frequent mutations caused always the same +1 shift of the open reading frame, generating a new C-terminal sequence and determining the loss of KDEL domain. It goes without saying that the first hypothesis for CALR mutant effects was the delocalization of the protein, with an impairment of the ER retrieval pathway.

Later works explained the tight connection between CALR mutations and ET/PMF. The loss of ER retrieval signal and the novel peptide allows CALR to escape ER, strongly binding the TPOR/MPL . CALR-TPOR complex co-migrate on the membrane activating signaling towards megakaryopoiesis, which explains the higher frequency of CALR mutations in ET and PMF, an their apparent absence in PV[46-48]. Beyond such gain-of-function effect, few data have been collected about the hypothesis of a CALR physiological hematopoietic pathway disrupted by CALR mutations.

The experiments conducted by Di Pietra and coworkers investigated for the first time whether MPN CALR mutants affect the Calcium buffering in megakaryocytes of ET patients. In non excitable cells, many processes are regulated by cytoplasm Ca^{++} concentration $[Ca^{++}]_C$, which can dramatically change due to Ca^{++} flux from ER and, consequently, from the extracellular space, according the Store-Operated Ca^{++} Entry (SOCE). By blocking the main channel responsible for Calcium intake from cytosol to the ER, they measured the cytosolic Ca^{++} efflux, first from ER to cytosol, and then from extracellular space to the cell. It was observed that CALR type 1 mutation determines the highest Ca^{++} fluctuation, hypothesizing a higher rate of Ca^{++} binding for this variant, but the functional consequences on megakaryocytes signaling are unclear[49].

Robust data clearly support a gain of function for CALR novel C-terminal peptide in MPNs, with the activation of TPOR and JAK/STAT pathway, and answering most of the questions about a connection between this mutated protein and hematopoiesis. However, any aspect regarding regulation of CALR gene expression in MPN has been generally neglected, despite its expression levels have been measured in several types of cancers, resulting often upregulated, with some exceptions[50-52].

1.3.5 Regulation of gene expression.

Looking at the overall picture, CALR functions in physiological and pathological conditions are disparate, almost confusing. Noteworthy, against such multi-faced protein functions, even difficult to frame in a single main biological process, the studies conducted on the counterpart field of CALR expression regulation are surprisingly scarce. It is likely that the entireness of CALR tasks also depends on a fine transcriptional regulation, modulated in different contexts. CALR promoter has been analyzed, reporting several potential transcription binding sites, whose activation is mainly related to a Ca^{++} response in the context of embryogenesis and particularly cardiogenesis. For some of these transcription factors, such as Nkx2.5, GATA6, Evi-1 and MEF2C, a regulating activity has been experimentally proved[26, 53, 54]. In some cases CALR appeared even to control in turn the regulation exerted from such transcription factors. However, all these studies are limited mainly to mice cardiogenesis, and should require further investigations.

1.3.6 CALR 3'UTR.

Experimental data on the post-transcriptional regulation are even more lacking. Few papers focused on this aspect of CALR modulation, with findings regarding the miRNA miR-455.3p involved in CALR repression within the context of heart hypertrophy and ischemic damage protection mediated by ER stress response[55, 56].

Although the evidences of CALR expression regulation are limited to the context of cardiac development and physiology, it is reasonable that a gene so widely expressed across diverse tissues and functionally multiform might have a robust regulative apparatus, which still need to be clarified. In this sense an interesting work from Vuppalanchi et al., demonstrated how two conserved regions of CALR 3'UTR are required to localize the relative transcript in axons of murine neurons, moving the protein synthesis distant from soma. Precisely, by FISH experiments they

demonstrated that CALR mRNA is localized to axons, and so the protein; then by expressing a GFP mRNA bearing the 3'UTR of CALR, they showed how the mRNA and the fluorescent protein were localized in the axons, and the specific removal of such 3'UTR sequences induces the loss of axon localization for GFP-CALR-3'UTR, both for mRNA and protein[57].
This paper open the door towards a field not yet considered. The 3'UTR mRNA sequence of CALR might be engaged for specific process, regulating at various levels the multiple functions of these protein, even in those still unclear pathological milieu such MPNs.
Moreover, despite the authors did not investigated the RNA binding proteins responsible for such mRNA localization, these data can be placed on a broader context that assigns increasing functional roles to the non-coding regions of mRNA, one of which is transcript localization, driven by specific in-cis sequences of 3'UTR, as will be discussed later.

1.4 3'UTR functions

Over decades, researchers relied on protein the core of all essential functions within cells. The possibility to fold and organize in various secondary, tertiary and quaternary structures, either with the post-translational modifications to higher degree of complexity, explains all various functions of proteins, both structural and enzymatic. Later became clear that RNA deserved increasing importance. Originally the only characterized class of this molecule was messenger RNA (mRNA), encoding for proteins and allowing their synthesis, and thus considered just as intermediary of genetic information. Now RNAs have been widely classified in many classes, depicting an intricate mosaic of functions. For instance, ribozymes demonstrated how the complexity of an RNA molecule could compete with that of protein enzymes. Intimately interacting with proteins, some RNAs form a particular class of molecules known as ribonucleoproteins (RNPs), acting on crucial cell functions such as protein synthesis, mRNA processing and DNA damage protection. Moreover, regulation of gene expression

lays on a large part on various classes of RNAs. Thus RNAs have a great functional potential, only partially explored. As the central dogma states, the function of mRNA is to codify the gene information that is translated into protein. Nevertheless, the structure of a mature mRNA entails regions that do not codify for translation, thus untranslated, placed at the 5' and 3'ends of the transcript, flanking the central coding sequence. Such regions initially thought to be devoid of significance, have now acquired increasing functional importance.

1.4.1 Mechanisms of 3'UTR physiological functions.

The 3' untranslated region (3'UTR) is the sequence of an mRNA transcript that follows the stop codon. Localized at the end of the last exon, it is part of the mature transcript although it is not translated into protein. Albeit being a non-coding sequence, it contains crucial regulative elements. It is widely known that miRNAs guide the Argonaute proteins in specific sites of 3'UTR, thus inducing degradation of the mRNA or inhibition of its translation[58]. In addition, unexpected functions for this non-coding region of mRNAs are emerging recently[59] (fig. 1.4).

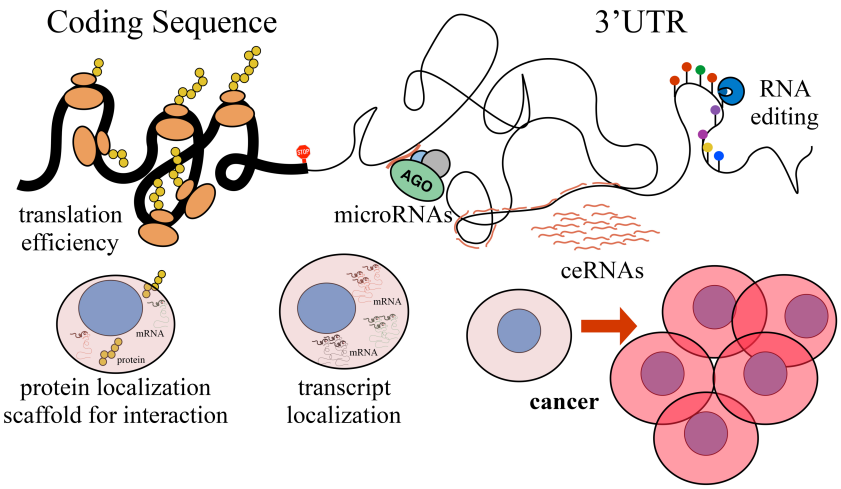

Figure 1.4. Novel functions of 3'UTR. Recent findings highlight new roles of 3'UTR are summarized in the diagram (see text for details). 3'UTR are reported

to affect protein translation efficiency; 3'UTR shortening determines modulation of microRNA binding, inducing miRNA-repression escape and affecting ceRNA crosstalk; moreover 3'UTR modulates transcript and protein localization. All these mechanisms might be involved in cancer, where recent works frequently reported that crucial gene of cancer are highly expressed after 3'UTR deletions or disruption.

In neuronal model systems, various experimental works have proven that 3'UTR are necessary for differential transcript localization between soma and axon. Brain-derived neurotrophic factor (BDNF) is transported along actin fibers through RNA binding proteins (RBPs) that recognize specific regions within the 3'UTR[60]. By RNA-seq it has been demonstrated that 3'UTR are required to localize transcripts at neuritis, by means of a mechanism relying on the RBP Muscleblind-like protein (Mbnl)[61]. In the same tissue, it has been previously mentioned the evidence that in-cis sequences of CALR 3'UTR are capable to determine the transcript localization, forcing the protein synthesis to be carried out directly at the axon, far from soma[57].
Also translation efficiency is affected by 3'UTR, as showed during drosophila development, in which the protein Polo has to be expressed in high quantity to permit the proliferation of abdominal epidermis precursor cells. It has been showed that 3'UTR of Polo mRNA is required for translation at high rates[62]. More intriguingly, 3'UTR may act as scaffold for protein interaction. A recent experimental work indicated that during its protein synthesis, CD47-long UTR is essential for interaction with Human antigen R (HuR) and SET, thereby recruiting Ras-related C3 botulinum toxin substrate 1 (RAC1) and mediating the translocation of nascent protein to the plasma membrane. This mechanism seems to be valid for other plasma membrane proteins, furnishing a new paradigmatic model of protein localization, dependent by 3'UTR[63]. This localization plasticity allows CD47 to transduce an anti-phagocytic signal when it is expressed on the cell surface for the self-recognition by immunity system. Such mechanism has been employed also to specifically target phagocytosis towards Acute

Lymphoblastic Leukemia cells (ALL) by using monoclonal antibodies[64]; it is quite interesting to notice that CALR analogously migrates on cell membrane, antagonizing CD47 signal and operating as a pro-phagocytic signal, as previously discussed, although it is not known through which mechanisms this migration of CALR on cell surface is conducted.
Strikingly, cited and other mechanisms 3'UTR-dependent were only partly elucidated so far and are involved in master process of cell biology and, more importantly, in disease.

1.4.2 Functional roles of 3'UTR in cancer
An endless bulk of data supports the roles of mi-RNAs in tumors. Within the context of all recently highlighted 3'UTR functions, miRNA regulation can be rethought, linking it with another crucial molecular event, Alternative Polyadenilation (APA). Since 3'UTR bear usually negative regulative elements, the loss of sequence traits as consequence of deletion or APA subtract the mRNA to the control of negative effector such as miRNA, escaping from repression[65], leading to an increased expression of the related gene, a mechanisms known as 3'UTR shortening[66]. This process is intimately dependent from APA, in various and contrasting fashions. Recent works demonstrated that more effective miRNA binding sites are positioned at the extreme ends of 3'UTR (immediately downstream the stop codon or close to the poly-A site)[67, 68]. By RNA-seq it was showed that miRNA binding sites are enriched specially in proximity to APA sites of oncosuppressor genes; these APA sites are physiologically latent but, in cancer cells, the APA could be up-regulated, bringing these miRNA binding sites at the end of 3'UTR transcript, which is therefore shorter than previously. By this mechanism, the transcript is thus highly repressed, favoring the status of de-differentiation/proliferation[69]. In the end, 3'UTR shortening has been associated to the peculiar class of Competitive Endogenous RNA (ceRNA), that bind high levels of miRNAs, regulating their free and sequestered fractions. It has been showed that ceRNAs are

particularly affected by 3'UTR shortening, and this free-up high levels of miRNAs, that target the other ceRNA partners, generally tumor suppressor, and compromise their crosstalk, repressing them and promoting tumor growth. Importantly, 3'UTR disruption might occur as well as result of deletions[70]. In some cases, even the expression of a specific RBP could affect the levels of its mRNA target. Recently it has been demonstrated in breast cancer that the nucleus-cytoplasm shuttle Vigilin bind a 69 bp 3'UTR sequence of Colony Stimulation Factor Receptor (CSF-1R), a tyrosin-kinase involved in breast cancer metastasis and survival, thereby inhibiting its translation. The expression levels of vigilin are high in normal tissues and reduced in cancer[71]. The gene Programmed Death Ligand-1 (PDL1), which mediates immune escape of several cancer, it has been found overexpressed in a series of tumors and is associated with the evasion from immune response, and this effect is determined by PDL1 3'UTR disruption[72]. Interestingly, a recent study on cyclin D1 isoforms showed that shortened isoform of Cyclin D1 are associated with TP53 alteration and proliferation in Mantle Cell lymphoma[73]. All these data highlight a strong functional correlation between 3'UTR disruption and cancer.

A novel concept that completes the depicted scenario is the new field of "epitranscriptomics" that, analogously to epigenomics, dramatically extends the potential of a single nucleotide sequence. In fact the enzymatic modifications direct to RNA bases, known as editing, can modify the complementarity properties of RNA sequences and could further amplify the functional potential of non-coding regions[74]. Indeed 3'UTR are particularly enriched in editing modifications, respect to other regions of mRNA; more interestingly, not all transcript are affected by editing, indicating that this could be a mechanism to diversify the effector possibilities of mRNA sequences. Recently adenosine-to-inosine editing by adenosine deAminase acting on RNA (ADAR1) has been founded activated in blast crisis of CML[75]. Importantly, a study conducted in mice proven that the homozygous KO of

ADAR1 is lethal for embryos, while heterozygous dies at day 14 due to an impairment of erythropoiesis[76]. Lastly, all this data could be related to another property of RNAs. Indeed it is clearly recognized that RNA folds in specific secondary structures, which might be at the basis of RBP binding, but only few domains and principles governing these interactions have been identified so far[77].

It is broadly accepted that high eukaryotes complexity is given by non-coding regions rather than protein sequences[59]; in this sense 3'UTR might represent the submerged side of the iceberg, justifying the profound difference between organisms respect to a general genome similarity. However, despite the enormous potential of 3'UTR only partially sketched by these molecular mechanisms, its implication in crucial process of tissue homeostasis or development, such hematopoiesis, or multifactorial disease, such cancer, still need further investigation.

2. Aims

CALR is a multifunctional protein involved in a wide variety of cellular processes[23]. Its expression levels are increased in several cancers. However, the physiological role of CALR within the context of hematopoiesis is still poorly understood. In addition, CALR mutations have been found in MPNs, involving both the coding[78] and 3'UTR regions (by our group, this study, unpublished data). Recently, new functional roles of 3'UTR are emerging[79]. Specific region of CALR 3'UTR have been reported to impact on localization of mRNA and translation site. Generally 3'UTR disruption have been associated to the upregulation of several crucial genes in cancer[80].
Based on these findings the aims of the project were:

2.1 - To investigate the putative role of CALR in hematopoiesis. The kinetics expression of CALR during physiological hematopoiesis and MPNs were investigated by employing unilineage cultures of HSCs, an in vitro model of myelopoiesis.

2.2 - To elucidate the function of novel mutated variants of CALR 3'UTR in pathological myelopoiesis (MPNs).
The mutational status of CALR was analysed in a large cohort of MPNs patients. By extending to CALR 3'UTR region the research of CALR mutational variants, routinely limited on CALR exon 9 coding sequences, we identified and functionally characterized novel alterations affecting the 3'UTR region of CALR.

2.3 - To realize a model in vitro to study the functional consequences of CALR 3'UTR disruption in myelopoiesis. CRISPR CAS9 technology was used to remove specific sequences of CALR 3'UTR in myeloid progenitors in order to observe any effect in myeloid differentiation.

3. Materials and methods

3.1 Patients and healthy donor samples.

Peripheral blood buffy coat specimens were collected from informed healthy donors and patients according to ethical issue agreement with the UOC Ematologia, Ospedale S.M. Goretti (Latina).

3.2 PBMCs isolation.

Per each patient, about 20 ml of peripheral blood (PB) were transferred in sodium-citrate tubes and centrifuged 1200 rpm for 10 minutes. Then buffy coat was recovered and resuspended in 10 ml of EL-ERythrocytelysis buffer (Qiagen) for erythrocytes lysis, then centrifuged again and resuspended in 1 ml of Phosphate Saline Buffer (PBS) for cell count and eventually stored at -20˚C as dry pellet.

3.3 Cell lines.

Myeloid cell lines K562, and CRISPR CAS9-gene edited K562 (see below) were all maintained in RPMI 1640 + GlutaMax medium, supplemented with 10% Fetal Bovine Serum (FBS), 50 μg/ml streptomycin and 50 IU/ml penicillin. All cell lines were cultured in a fully humidified incubator with 5% CO2 in air.

3.4 DNA extraction.

DNA was extracted from peripheral blood buffy coat or cell lines by salting out method as previously described[81]. The buffy coat-derived dry pellets were digested overnight at 37° C with 3 ml of Lysis buffer (0.01 M Tris-HCl pH 8.2, 0.25 M NaCl, 0.5% 2 mM EDTA, 1% SDS) and 1 mg/ml protease K (Ambion). After complete digestion, 800 μl of 5 M NaCl was added to each tube and vortexed vigorously for 15 sec, followed by centrifugation at 2500 rpm for 15 min. The supernatant containing the DNA was transferred to a new tube and precipitated with 100% ethanol; samples were centrifuged at 2500 rpm for 15 minutes and DNA

pellet was washed 3 times with 70% ethanol and then air-dried. DNA pellet was resuspended in TE buffer. DNA concentration and purity were analyzed by spectrophotometer and then ran on 1% agarose gel.

3.5 PCR, Sanger Sequencing and Fragment Analysis.
CALR exon 9 mutations were assessed by qualitative PCR and agarose gel, by using forward CCTGCAGGCAGCAGAGAAAC and reverse ACAGAGACATTATTTGGCGCG primers[82]. Detected mutations were identified by Sanger sequencing using the same primers and confirmed for size of insertion or deletion by fragment analysis, performed with forward CTGGTCCTGGTCCTGATGTC labeled with 6-FAM™ and reverse CGAACCAGCCTGGAAAAA primers[83]. From fragment analysis, allelic burden was calculated by intensity of FAM fluorescence for mutated and wild type alleles [mutated/(mutated + wild type) x 100]. PCR-derived samples for sequencing and fragment analysis were processed by BioFab Research srl facility (Rome, Italy).

3.6 Clustal Omega aligments.
CALR protein and 3'UTR mRNA sequences were selected from following 9 vertebrate species: Human - *Homo sapiens* (NP_004334-NM_004343), rhesus monkey - *Macaca mulatta* (NP_001248060-NM_001261131), mouse - *Mus musculus* (NP_031617- NM_007591), Norway rat - *Rattus norvegicus* (NP_071794- NM_022399), cattle - *Bos taurus* (NP_776425-NM_174000), Horse - *Equus Caballus* (XP_001504932-XM_001504882), chicken - *Gallus gallus* (XP_025001564-XM_025145796), dog - *Canis lupus familiaris* (XP_867310-XM_862217), Tropical clawed frog - *Xenopus tropicalis* (NP_001001253- NM_001001253). For each mRNA sequence, the region comprised within first 100 nucleotides of each 3'UTR sequences was taken into account, whereas for proteins the aminoacids included within last 60 residues were chosen. Both

groups of sequence were submitted to Clustal Omega multiple sequence alignment (https://www.ebi.ac.uk/Tools/msa/clustalo/). The output of alignment was elaborated with Jalview v 2.10.4.

3.7 Immunoblotting.
For immunoblotting assays total proteins from cell extracts were quantified by the Lowry Protein Assay[84] and 40μg of total protein extract from each sample were fractionated on 4-12% SDS polyacrylamide gel and electroblotted onto a nitrocellulose membrane. Blots were probed with the following primary antibodies: anti-CALR from Millipore, anti-pSTAT5(Y694), anti-STAT5, anti-pSTAT3, anti-STAT3 and anti-GAPDH purchased from Cell Signaling. Secondary antibodies used were anti-mouse IgG and anti-rabbit IgG horse radish peroxidase conjugate (BioRad). Immunoreactivity was detected using the ECL method (Amersham Biosciences).

3.8 Clonogenic assay.
The colony assays were performed using peripheral blood mononuclear cells from patients using the MethoCult^{TM} medium (Stem Cell Technologies, Vancouver, British Columbia, Canada) according to the manufacturer's instructions. Briefly, $2x10^5$ PB (peripheral blood) nucleated cells were suspended in 1 mL methylcellulose medium supplemented with SCF, GM-CSF, IL-3, and EPO 3 U/ml (Methocult H4034), or in methylcellulose medium containing SCF, GM-CSF and IL-3 (Methocult H4035) supplemented with EPO at final concentration of 1 or 0.1 U/ml, and plated in 35-mm culture dishes. After 14 days, each plate was scored for erythroid Burst Forming Unit (BFU-E) or Granulocyte-Monocyte Colony Forming Unit (CFU-GM) growth.

3.9 Flow cytometry.
K562 cells were analyzed using FACS CANTO II (Becton Dickinson San Jose CA,USA), and data were analyzed using FACS DIVA software. Antibody staining was performed as

follows: $1x10^5$ cells were incubated for 10 minutes at room temperature, and then washed with PBS containing 0.1% sodium azide (Becton Dickinson). For HSPC markers, cells were stained with a PE-Cy7 conjugated anti-human CD117 (Becton Dickinson), PerCP-Cy5.5 conjugated anti-human CD34 (Becton Dickinson). To analyse myeloid cell lineage markers, cells were stained with a FITC-conjugated anti-human CD15 (Becton Dickinson), FITC-conjugated anti-human CD 14 (Becton Dickinson), PE-conjugated anti-human CD64 (Becton Dickinson), PE-conjugated anti-human CD11b (Becton Dickinson), FITC-conjugated anti-human CD 61 (Becton Dickinson). To analyze erythroid cell lineage markers, cells were stained with a PE-conjugated anti-human Glycophorin A (CD235a) (Becton Dickinson), APC-conjugated anti-human CD71 (Becton Dickinson).

3.10 CRISPR-CAS9 constructs design and transduction.

To reproduce patient's mutation CRISPR/CAS9 constructs were used to generate 24bp deletion on CALR 3' UTR. LentiCRISPRv2 puro was a gift from Dr. Feng Zhang through Addgene (plasmid # 52961)[85, 86]. sgRNAs sequences were designed using the web-based program CRISPR DESIGN[87] (http://crispr.mit.edu/). Two sgRNAs were used in this study: sgRNA1 and sgRNA2. These two sequences were synthesized (Eurofins Genomics) as 5'phosphorylated-oligonucleotide pairs (Table 1). Each oligonucleotide carried extra bases to allow the cloning of the target sequences at the BsmBI site located after the U6 promoter of the vector lentiCRISPRv2 puro. All the cloning steps were done using protocols, available on the Addgene website (www.addgene.org)[85] and the constructs were verified by sequencing. Vectors for genome editing and the empty vector, used as control were transferred to K562 cells by lentiviral transduction. Lentiviral particles were produced as published[88]. The cells were selected in 2 µg/ml puromycin and single clones were isolated by limiting dilution.

3.10.1 Mutations analysis

Puromycin-resistant clones were screened for CRISPR-mediated deletions by PCR amplification/sequencing. Genomic DNA from each clone was extracted using the QuickExtract DNA Extraction Solution (Epicentre) following the manufacturer's protocol. Briefly, pelleted cells were resuspended in QuickExtractsolution, incubated at 65°C for 6 minutes and at 98°C for 2 minutes. Lysate was used for target region amplification. Polymerase chain reaction (PCR) was performed using a set of primer outside the sgRNA recognition sites to amplify a 225 bp region (Table 1). The fragments with the intended deletion were evaluated by size against the wild type and vector fragments by gel electrophoresis. To confirm the mutations, DNAs were used for a second PCR amplification in a negative screening where the reverse primer was included in the deletion (Table 1). In these conditions the putative intended deletion would disrupt the amplification or would produce a weak amplicon in the heterozygous clones. All PCR reactions were carried out using the High-Fidelity DNA polymerase (Thermo Fisher Scientific). The putative mutant DNAs were purified with HiYield gel/pcr DNA fragments extraction kit (RBC Bioscience) and sequenced by direct Sanger-sequencing at Eurofins Genomics.

sgRNA and Primers	Function	5' to 3' sequence
sgRNA 1	Targeting CALR gene	CTCAGTCCAGCCCTGGAGGC
sgRNA 2		CTGCCTCCAGGGCTGGACTG
Primer sgRNA 1 For	Cloning sgRNA1 in pLentiCRISPRv2	CACCG CTCAGTCCAGCCCTGGAGGC
Primer sgRNA 1 Rev		AAAC GCCTCCAGGGCTGGACTGAG C
Primer sgRNA 2 For	Cloning sgRNA2 in pLentiCRISPRv2	CACCG CTGCCTCCAGGGCTGGACTG
Primer sgRNA 2 Rev		AAAC CAGTCCAGCCCTGGAGGCAG C
Primer C For	Detecting CALR 3'-UTR deletions	CAAGGAGGATGATGAGGACAAA
Primer C Rev		CCAAATCCGAACCAGCCT
Primer F For	Confirmation screening of mutant clones	GCAGAGAAACAAATGAAGGACAAA
Primer F Rev		GCTCAGGCCTCAGTCCA

Table 3.1: Primers sequences for single guide cloning and mutations validation. sgRNA 1 and sgRNA 2 sequences are designed to target the human CALR 3'-UTR. Primers sgRNA 1 and primers sgRNA 2 were used for cloning guides in pLentiCRISPRv2 puro. Primers C were used to amplify a 225bp region around the sgRNA 1 and the sgRNA 2 recognition sites for detecting the intended deletion. Primers F were employed in the negative screening of putative mutant clones with the reverse primer included in the deletion.

3.11 RNA extraction, cDNA synthesis and RT-PCR.
Equal amounts of RNA (1 μg) were reverse transcribed into cDNAs with random hexamers and MuLV reverse transcriptase (Applied Biosystems). CALR, GAPDH or HPRT1 mRNAs were measured by quantitative RT-PCR in the ABI-PRISM 7000 (Applied Biosystem). The relative quantity of mRNA was calculated by $2^{-\Delta Ct}$ method.

3. 12 Droplet digital PCR for JAK2V617F mutation detection.
The digital PCR (ddPCR) assay was performed with the PrimePCR™ ddPCR™ Mutation Detection Kit Assay for JAK2 wild-type and the V617F mutation (Bio-Rad Laboratories, GmbH, Munich, Germany). The wild-type and V617F mutation probes were labeled with either the HEX or FAM fluorochromes, respectively. The ddPCR reaction volume was 20 μL and composed of 10 μL of ddPCR supermix for probes (no dUTP) (Bio-Rad), 1 μL of target and reference amplification primers/probes mix and 40ng of DNA template. Each reaction mixture was partitioned into approximately 20,000 droplets by the QX200 droplet generator machine. 40μl of generated droplets were placed into a PCR 96-well plate (Bio-Rad). Plates were sealed using pierceable foil heat seal and a PX1 PCR plate sealer (Bio-Rad) and then cycled under the following conditions: 10 min at 95 °C, 30 s at 94 °C and 1 min at 55 °C for 40 cycles with a ramp speed of 2 °C/s, 98 °C for 10 min, and hold at 4 °C. Cycled droplets were read in the QX200 droplet-reader and analysis of the ddPCR data was performed using the QuantaSoft analysis software (Bio-Rad). The threshold between the positive and negative droplet clusters was manually set for both FAM and HEX channels for each sample. The fractional abundance of V617F mutation was calculated by the software as follows: V617F positive droplets/(V617F positive droplets + wild-type positive droplets) ×

100. ddPCR data presented are indicated as V617F fractional abundance ± Poisson 95% confidence intervals.

3.13 Droplet digital PCR for miRNA expression

To evaluate miR455.3p and mir1972 expression in either cell lines or patient samples droplet digital PCR (ddPCR) was performed according to manifacture's instruction on the QX200 ddPCR system (Bio-Rad), using TaqMan MicroRNA assay specific for hsa-miR-101 (Applied Biosystem). 20µl reactions were assembled with 2µl miR-specific cDNA, 1× TaqMan MicroRNA Assay (forward primer, reverse primer, and probe), and 1×ddPCR supermix for probes (no dUTP) (Bio-Rad) in 20 µl of reaction volume that was loaded into droplet generator cartridges with 70µl droplet generation oil for probes (Bio-Rad). Each reaction mixture was partitioned into approximately 20,000 droplets by the QX200 droplet generator machine. 40µl of generated droplets were placed into a PCR 96-well plate (Bio-Rad). Plates were sealed using pierceable foil heat seal and a PX1 PCR plate sealer (Bio-Rad). A PCR was performed on the T-100 thermal cycler (Bio-Rad) under the following conditions: 10 min at 95 °C, 30 s at 94 °C and 1 min at 60 °C for 40 cycles with a ramp speed of 2 °C/s, 98 °C for 10 min, and hold at 4 °C. Droplet were evaluated using the QX200 droplet reader machine and QuantaSoft Software (Bio-Rad). The threshold between the positive and negative droplet clusters was manually set for each sample. ddPCR data presented are indicated as absolute copies of transcripts per µl of reaction sample ± Poisson 95% confidence intervals.

3.14 Human peripheral blood (PB) hematopoietic progenitor cell (HPC) purification, suspension culture and unilineage culture. PB low-density mononuclear cells were isolated by Ficoll–Hypaque density gradient centrifugation (Pharmacia). CD34+ cells were purified by positive selection using the midi-MACS immunomagnetic separation system (Miltenyi Biotech) following the manufacturer's recommendations. The purity of

CD34+ cells was assessed by flow cytometry and was routinely over 95%. CD34+ HPCs were cultured in a fully humidified 5% CO2, 5% O2 atmosphere, in serum-free medium and passaged at 2 x 10^5 cells/mL. Serum-free medium was prepared as follows: freshly prepared Iscove's modified Dulbecco's medium (IMDM) was supplemented with: bovine serum albumin (10 mg/mL), pure human transferrin (700 μg/mL), human low density lipoprotein (40 μg/mL), insulin (10 μg/mL), sodium pyruvate (10^{-4} mol/l), L-glutamine (2 x 10^{-3} mol/l), rare inorganic elements supplemented with iron sulfate (4 x 10-8 mol/l) and nucleosides (10 μg/mL each). The following cytokines were added: Epo (3 U/mL), IL-3 (0.01 U/mL) and GM-CSF (0.001 ng/mL) for erythroid (E) unilineage culture; for granulocytic (G) culture serum free medium was supplemented with IL-3 (1 U/mL), GM-CSF (0.1 ng/mL), and G-CSF (500 U/mL).

3.15 Immunofluorescence and video-confocal analysis.

Subcellular localization of CALR was investigated in Methanol-Acetone fixed and permeabilized cells from BFU-E and CFU-GM colonies obtained from PB of healthy donors and patients, using anti-CALR antibody (Millipore) or anti-Golgin (Abcam). AlexaFluor488 donkey anti-rabbit was used as secondary fluorescent antibodies. Cells were counterstained with DAPI. The slides were coverslipped using Vectashield anti-fade reagent. 3D and Z-stacked images were obtained using the Nikon ViCO videconfocal microscopy with a 63X oil objective and analyzed with NIS-Element viewer (Nikon).

3.16 Statistics

The analysis of experimental data by descriptive statistic was performed using GraphPad Prism 7. The one-way ANOVA with Turkey's post test was employed to analyze CALR mRNA levels in cord blood unilineage culture. Pearson correlation index was used to measure the correlation between mRNA levels and genomic allele burden of CALR in MPNs patients. Two-tailed test

was employed in evaluating control, PV and single patient's CD34+ unilineage cultures. A p value <0.05 was considered as index of statistical significance.

4. Results

4.1 CALR expression in physiological and pathological hematopoiesis.

The first aim of this project was to evaluate whether in physiological hematopoiesis CALR shows a lineage-dependent gene expression. Furthermore, CALR mutants have been identified in MPNs, a pre-malignant condition with overproduction of myeloid series, mainly erythroid and megakaryocytes lineages. Thus we aimed also to evaluate expression levels of CALR in the context of pathological hematopoiesis, relating them to the mutational status of CALR.

4.1.1 CALR mRNA is barely expressed during erythroid and megakaryocytic differentiation, and highly during granulopoiesis and monopoiesis.

By using unilineage cell culture of cord blood $CD34^+$ HSCs as an in *vitro* model of myelopoiesis, we measured mRNA levels of CALR along all 4 myeloid lineages (fig. 4.1.A). CALR mRNA showed a peak at day 6 of granulocyte differentiation, then decreasing until day 8; monocyte differentiation follows the same kinetics, but at lower expression levels. By contrast, no main fluctuations are observed along erythroid and megakaryocytic lineages, where CALR expression is substantially kept constant and inferior respect to granulo-mono routes. Importantly, ANOVA analysis with Turkey's multiple comparisons test confirmed that granulocytic and erythroid CALR mRNA levels significantly differs at day 6 and 8 of differentiation ($p<0.0001$); at the same days a similar difference is reported between granulocytic and megakaryocytic mRNA amounts ($p<0.001$). Conversely, CALR mRNA of erythroid and megakaryocytic differentiation do not significantly differ.

An indirect confirmation of such finding about granulocytic lineage was observed by immunofluorescence of CALR protein in mobilized peripheral blood cells of healthy donors. Due to the

effect of stimulating factors, in these samples is possible to observe progenitor cells together with differentiate elements. In fact, granulocyte progenitors, resembling to myelocytes, have much higher expression of CALR, compared to differentiated granulocytes (fig. 4.1.B).
These data indicate that CALR is differently expressed through myelopoiesis, suggesting a lineage-specific modulation.

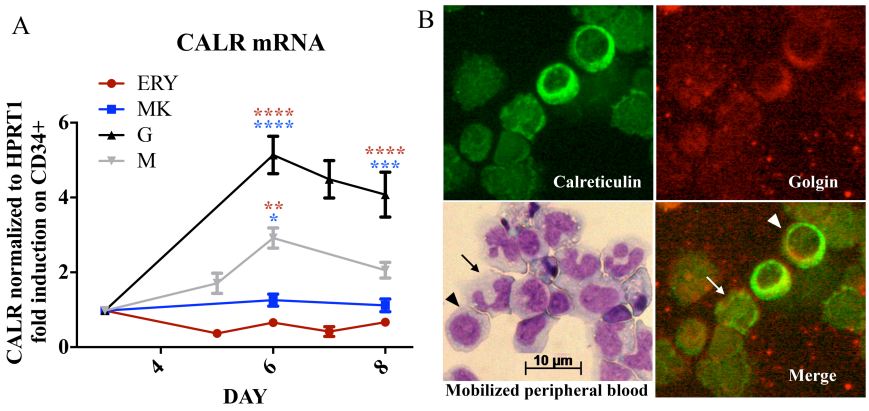

Figure 4.1. CALR is barely expressed during erythroid – megakaryocytic differentiation, and at high levels during granulo-monopoieis. (A) CD34+ unilineage liquid culture of cord blood CD34+, driven to erythroid, megakaryocytic, monocytic and granulocytic differentiation. CALR mRNA levels are normalized on HPRT1 and expressed by ΔΔ ct, as fold induction of each point respect to the day 0 (CD34+). Statistical analysis performed with ANOVA and Turkey's multiple comparison test. Red and blue stars indicate significance of granulocytic/monocytic vs erythroid and megakaryocytic lineages, respectively. (B) Wright-Giemsa morphology and immunofluorescence analysis of mobilized peripheral blood. Cells were stained with anti-CALR, in green fluorescence, and anti-Golgin in red fluorescence. Arrows indicate mature granulocytes, arrowheads point mielocytes. Cells were imaged in bright field and fluorescence at 40X objectives.

4.1.2 Identification of uncommon CALR mutations in MPNs associated to aberrant erythrocytosis (Polycythemia Vera).
CALR is mutated in MPNs, mainly exclusively in ET and PMF, which are diseases associated to abnormal megakaryopoiesis. The

most frequent CALR mutations are a 52 bp deletion (c.1099_1150del52/L367fs*46) and a 5 bp insertion (c.1154_1155insTTGTC/K385fs*47), named type 1 and type 2 respectively. In general, CALR mutations are a wide variety of deletions, insertions or indel in exon 9, all of which determine systematically the same 1-bp frameshift, generating a novel peptide, as shown in figure 4.2. The novel peptide has been reported to cause a CALR gain of function, with binding of TPOR and induction of megakaryopoiesis, leading to ET and PMF[46-48]. However, CALR mutations are commonly absent in PV. In a single institution study with a cohort of 286 MPN patients, we identified 3 non-canonical mutations in PV cases (fig. 4.3). The diagnosis of PV requires at least 3 major criteria, that are hemoglobin > 165 g/L or hematocrit > 49% (for men), a bone marrow with erythroid, granulocytic and megakaryocytic hypercellularity and the mutated status of JAK2 (JAK2^{V617F}). The clinical features of pt#1, pt#2, and pt#3 were compatible with a diagnosis of PV, as showed by values of hemoglobin, hematocrit, platelet and leukocytes (Table 4.1).

Figure 4.2. Schematic representation of canonical CALR mutation in ET and PMF. CALR WT and some of mutated variant commonly associated to MPNs (ET and PMF) are illustrated. For WT and each mutated variant, protein (aa 365-417) and mRNA (nt 1173-1331) are shown. The region of each mutation on RNA is highlighted by black box. Deleted nucleotides are red strikethrough, whereas insertions are in red. Deleted amminoacids are represented by gaps and mutated peptides generated by +1 frameshift are in red. Triplets within black

boxes and the stop sign symbol represent stop codons. The regions within the red square indicates the common novel peptide observed in CALR mutated MPNs. Besides the lost of KDEL domain, depicted by green box, an interesting consequence of such alteration is the conversion of the first 31 nt of 3'UTR in to coding sequence, a region indicated by black square. Type 1 – like and type 2 – like (T1-like, T2-like) and "others" are categories of classification described by Pietra et al.[49], according to the WT acidic domains lost in each mutation.

Clinical features of PV patients bearing uncommon CALR mutations			
Patient code	pt#1	pt#2	pt#3
Hemoglobin (g/L)	177	180	167
Hematocrit (%)	52	54	51.3
Platelets (10^9/L)	181	266	300
white blood cells (10^9/L)	8.9	11	4.4

Table 4.1. Clinical features of PV patients presented in this study are reported. Values are intended at the time of diagnosis.

The bone marrow biopsy complied with a histological pattern of PV (data not showed). However, the JAK2 mutational status was wild type, either for V617F (fig. 4.3.A) and exon 12 (data not showed), thereby the third criterion for a PV diagnosis was missing. Although not indicated by diagnostic workflow, to complete every possible analysis on such peculiar patients, we evaluated CALR mutational status by qualitative PCR and two types of deletions were observed (fig. 4.3.B). The precise characterization of such mutations was then determined by fragment analysis and sequencing.

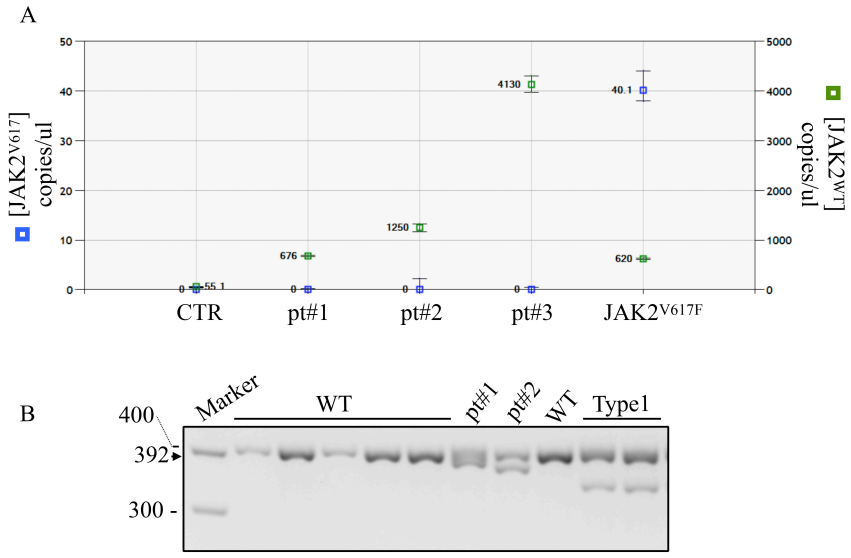

Figure 4.3. Pts#1, 2 and 3 are negative for JAK^{V617F} mutations, but were positive to qualitative PCR mutation assay for CALR. (A) Digital PCR with taqman assay on pts#1, 2 and 3. Healthy donor and JAK2^{V617F+} samples were employed as negative and positive controls respectively. (B) PCR assay and agarose gel conducted on pt#1 and pt#2. Multiple WT negative controls and CALR-type 1 deletion samples were loaded as size controls. Pt#1 and pt#2 presented deletions shorter than type1-del52, and were subsequently characterized as 12bp and 24bp deletions.

Patients #1, (pt#1) presented the mutation c.1214_1225del (E405_D408del), an in-frame 12 bp deletion of CALR C-domain, whereas patient #2 (pt#2) and patient #3 (pt#3) showed the variant c.1254+10_+33del, a 24 bp deletion located within CALR 3'UTR (fig. 4.4.A; interestingly pt#2 and pt#3 were siblings. Deletion c.1214_1225del was already described in PMF[89-91], whereas c.1254+10_+33del has been described by our group for the first time. Hereafter c.1214_1225del and c.1254+10_+33del are named del12 and del24 respectively. Both types of deletions do not alter the KDEL domain (fig. 4.4.B).

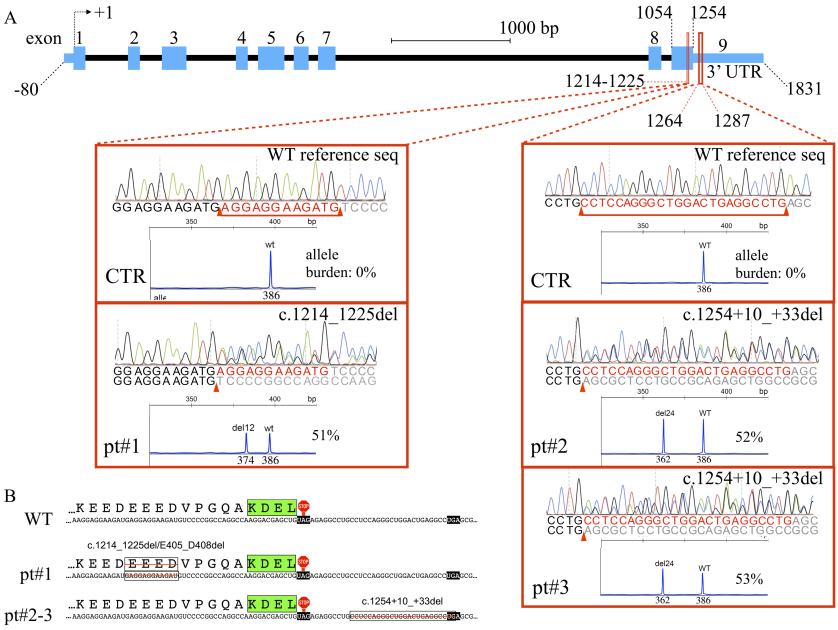

Figure 4.4. Identification of two non-canonical CALR mutations in PV-resembling patients. (A) Scheme of human CALR gene shows the structural organization of exons. Nucleotide number starts from the first base of coding sequence. Red inset indicates the region affected by the deletion. Fragment analysis and Sanger sequencing of genomic DNA show the size, allelic burden and region of deletions c.1214_1225del (del12) and c.1254+10_+33del24 (del24). Wild type reference sequence is employed to map deleted nucleotides in red, with red line and arrowheads, whereas sequence preceding and following mutation are respectively in black and gray. On mutated samples the junction is identified by red arrowhead. (B). Schematic representation of CALR mRNA region 1281-1371, comprising the sequence encoding for amminoacids K401-L417 of CALR C-domain, and part of the 3'UTR. Pt#1 harbors an in-frame 12bp deletion of coding sequence (c.1214_1225del), which causes the lost of amminoacid residues E405-D408 within the C-domain; pt#2 and pt#3 siblings show the mutation c.1254+10_+33del, a 24 bp deletion of 3'UTR. Interestingly the KDEL domain, indicated within green box, is retained in both types of mutations. Black boxes highlight stop codons; the stop sign labels the wild type canonical stop codon, while the unlabeled one is the stop codon of CARL common frameshift mutations in MPNs.

The mutations were assayed by Sanger Sequencing on DNA isolated from peripheral blood mononuclear cells (PBMCs), and then from CD34$^+$ cells, confirming the presence of del12 and del24 for all three patients. Both on PBMCs and CD34$^+$ cells, the allelic burden was equal or higher than 50% (fig. 4.5).
These data indicate that the mutated clones represented approximately half of peripheral blood cells population, supporting the presence of a clonal hematopoiesis. The familial relationship between pt#2 and pt#3 suggested that del24 could be a hereditary mutation. To address this matter we performed the genotype assay on saliva samples, detecting the same mutation with a similar allelic burden (fig. 4.5), indicating a potential inheritance of such mutation.

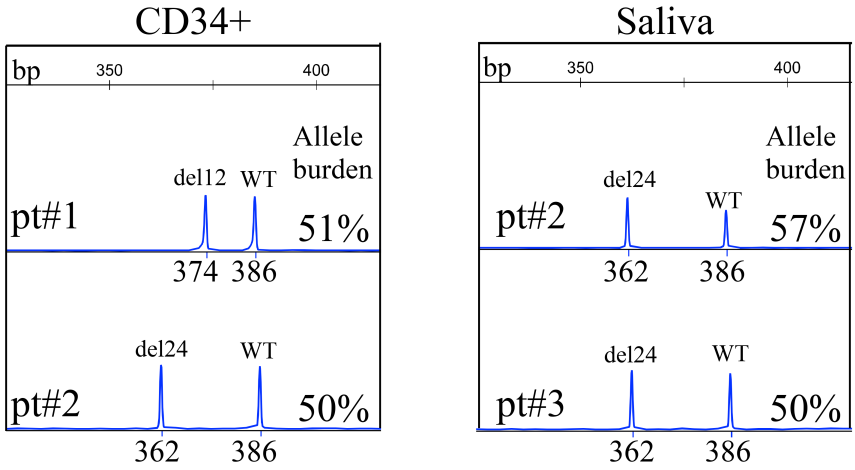

Figure 4.5. Del 12 and del24 are detectable in CD34$^+$ cells, and sibling pt#2 and pt#3 harbour del24 in saliva cells. Fragment analysis was conducted on DNA isolated from CD34+ cells of pt#1 and pt#2, and from buccal epithelium of pt#2 and pt#3. Allele burden of each variant was calculated as intensity of mut/mut + WT. The size of each allele is reported.

All these data demonstrated that non-canonical CALR mutations are present in patients with a PV phenotype. Such mutations do not alter KDEL domain but differently affect coding sequence and, more surprisingly, 3'UTR.

4.1.3 Unilineage cell culture and colony assay from pt#1,2,3 progenitors showed an erythroid growth propensity and megakaryopoiesis impairment.

To evaluate the differentiation properties of pt#1, pt#2 and pt#3 myeloid progenitor we performed unilineage cell cultures of $CD34^+$ cells isolated from pt#1 and pt#2, driving their differentiation towards erythropoiesis, megakaryopoiesis, granulopoiesis, and monopoiesis, and comparing them with unilineage cultures of $CD34^+$ cells isolated from healthy donors and from a group of PV bearing $JAK2^{V617F}$ mutation (fig 4.6-10).

Pt#1 progenitors showed an erythroid growth at low dose of EPO (0.1 U/ml), with a kinetics mainly overlapping to control PVs, whereas the growth curve at high dose of EPO (3 U/ml) was inferior to $PV^{JAK2V617F+}$, and more similar to that of myeloid progenitors from healthy donors. Conversely, megakaryocytic growth of pt#1 resulted analogous to that of $PVs^{JAK2V617F+}$. Particularly $PVs^{JAK2V617F+}$ megakaryocytes were significantly lower than healthy donors control at day 15, and megakaryocytes from PVs and pt#1 were both generally inferior to megakaryopoietic growth of healthy donors, whereas a slight increase was detected during monocytic differentiation respect to healthy donors and $PV^{JAK2V617F+}$ (fig. 4.6.A).

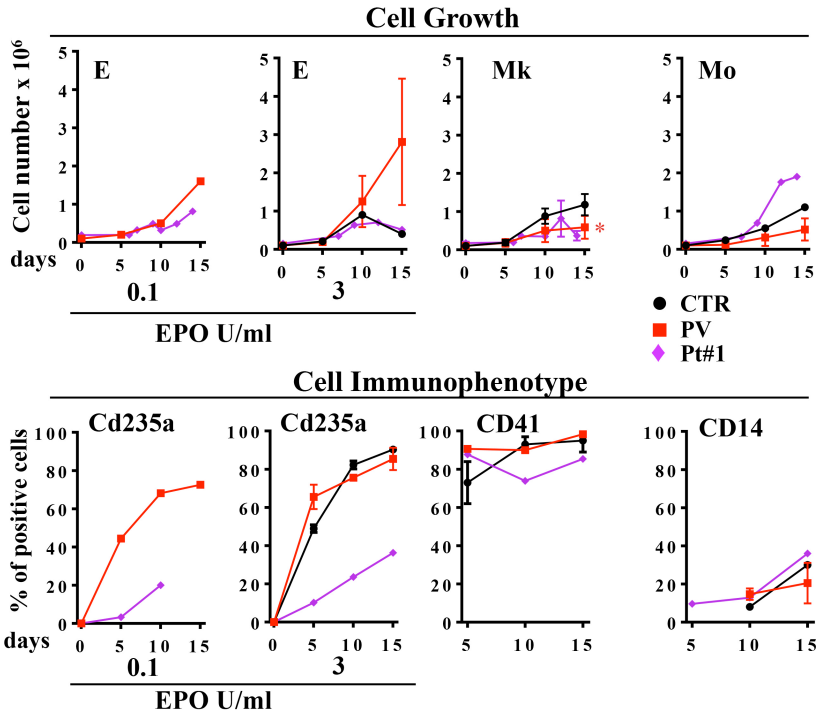

Figure 4.6. Unilineage cell cultures of pt#1 CD34$^+$ towards erythroid, megakaryocytic and monocytic lineages, and parallel monitoring of relative lineage markers. (A) CD34+ cells isolated from pt#1 were cultured under appropriate conditions towards erythroid, megakaryocytic and monocytic differentiation. Myeloid differentiation along such lineages was compared to the differentiation of CD34$^+$ from healthy donor (N=1) and PV^{JAK2V617F} (N=3), employed as controls. Erythroid growth was assessed at concentration of EPO 0.1 and EPO 3. Results are reported as number of cells per each culture at different days. Two tailed p value is indicated by * ($p<0.05$).
(B) Lineage specific markers assayed during CD34$^+$ unilineage cell cultures. CD235a (glicophorin A) measured erythroid differentiation, CD41 was employed to monitoring megakaryocytic differentiation and CD61 for monocytic differentiation. Data are shown as percentage of positive cells per each day.

Along the differentiation lineages we evaluated specific marker of myeloid differentiation (fig. 4.6.B). Although for pt#1 progenitor cells we observed erythropoiesis kinetics similar to control PVs

(EPO 0.1 U/ml), the levels of CD235a (glicophorin A), a specific marker of erythroid differentiation, increased along differentiation but at lower levels respect to PVs, at both tested EPO concentrations, and even lower than healthy controls. Interestingly, analyzing fluctuations of megakaryocytic marker CD41, impairment in megakaryocytic differentiation was observed respect to controls and PVs $^{JAK2V617F+}$; differently, no main changes were observed for CD11b, a marker of granulocytic and monocytic differentiation.
In contrast to pt#1, pt#2 showed a kinetic growth of erythropoiesis slightly inferior to PV$^{JAK2V617F+}$ at EPO 0.1 U/ml. However, pt#2 erythroid growth at EPO 3 U/ml was even greater than PVs at endpoint, indicating a strong growth potential through this lineage; differently from pt#1, pt#2 megakaryopoiesis did not substantially vary in growth respect to healthy donors; monocytes and granulocytes did not significantly differ among all 3 groups. (fig. 4.7.A).

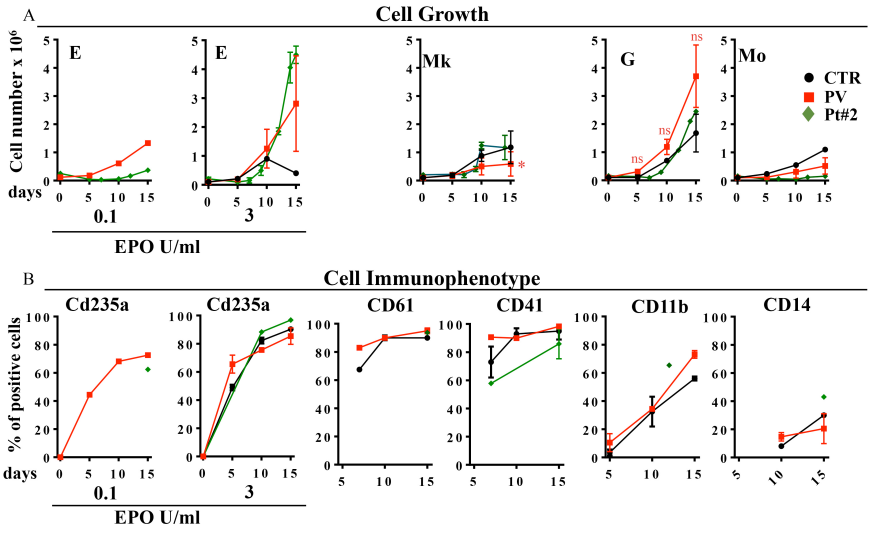

Figure 4.7. Unilineage cell cultures of pt#2 CD34^{+} towards erythroid, megakaryocytic and monocytic lineages, and parallel monitoring of relative lineage markers. (A) CD34+ cells isolated from pt#2 were cultured under

appropriate conditions towards erythroid, megakaryocytic granulocytic and monocytic differentiation. Erythroid growth was assessed at concentration of EPO 0.1 and EPO 3. N=4 $PV^{JAK2V617F}$ were employed as control, together with healthy donor (N=1). Results are reported as number of cells per each culture at different days. (B) Lineage specific markers assayed during $CD34^{+}$ unilineage cell culture of pt#2 of pt#1. CD235a (glicophorin A) measured erythroid differention, CD41 was employed to monitoring megakaryo differentiation and CD61 for monocytic differentiation. Data are shown as percentage of positive cells per each day. Two tailed p value is indicated by * ($p<0.05$).

As regard immunophenotypic markers, pt#2 had CD235a levels comparable to PVs $^{JAK2V617F+}$ and healthy donors, either at low and high EPO, indicating a high EPO sensitivity of pt#2 progenitors (fig. 4.7.B). Analogously to pt#1, a reduction of CD41 marker along megakaryopoiesis was present, while CD61 reached high levels, comparably to $PVs^{JAK2V617F+}$ and healthy donors. Pt#2 granulocytic CD11b and monocytic CD14 aligned to values of controls and PVs $^{JAK2V617F+}$.
In light of the alterations observed in erythroid and megakaryocytic lineages, we then dissected differentiation stages of erythropoiesis and megakaryopoiesis for pt#1 and pt#2 by measuring differentiating morphological subpopulations along unilineage cultures, and comparing them with erythropoiesis and megakaryopoiesis of healthy donors and $PV^{JAK2V617F+}$ (fig. 4.8).
The morphological analysis of distinct stages of differentiation highlighted that pt#1 CD34+ progenitor cells undergoing erythropoiesis entail the absence of proerythroblasts with a considerable increase of basophilic erythroblasts (fig. 4.8). Likewise pt#1, the erythroid population analysis of pt#2 showed lack of proerythroblasts, and a strong increase of basophilic erythroblasts as well, which recall a particularly accelerated maturation in that lineage, while polychromatophilic and orthochromatophilic erythroblasts remained generally constant (fig. 4.8, left panels).

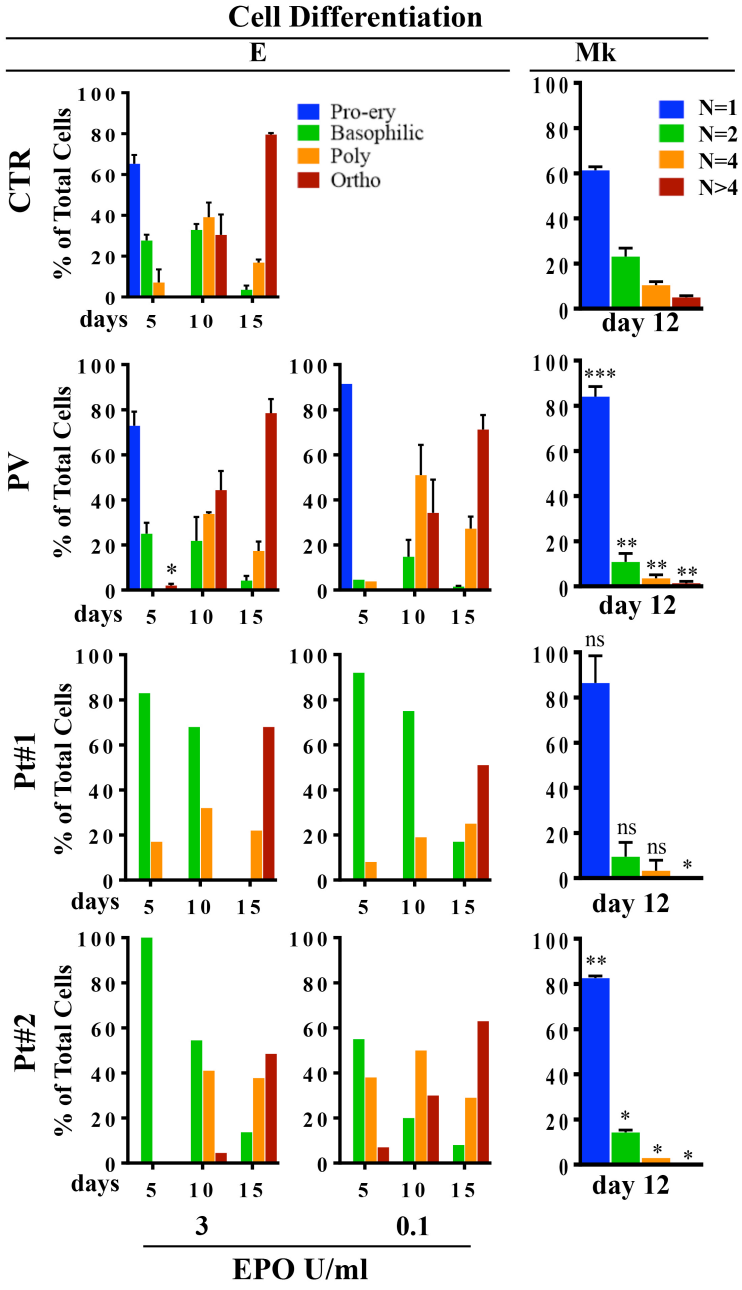
Cell Differentiation
E
Mk
CTR
PV
Pt#1
Pt#2
% of Total Cells
Pro-ery
Basophilic
Poly
Ortho
N=1
N=2
N=4
N>4
days
day 12
3
0.1
EPO U/ml

Figure 4.8 (previous page). Morphological analysis of erythroid and megakaryocytic populations along pt#1 and pt#2 CD34^{+} unilineage cultures. During erythroid and megakaryocytic differentiation cultures, cells were analyzed for their morphological subtypes populations of erythroid and megakaryocytic lineages. For erythroid differentiation, Pro-erythroblast, erythroblast basophilic, polychromatophilic and orthochromatophilic percentages are reported. As regard megakaryopoiesis, the percentage of mono and multinucleated (N=1, N=2, N=4, N>4) megakaryocytes at day 12 is reported as measure of megakaryocytic lineage maturation. Results are showed as percentage of population per each day. Student's t test was employed to compare every condition/day to the companion healthy donor control, and p values are reported (* = $p<0.05$, **=$p<0.01$, ***=$p<0.001$).

As regard megakaryopoiesis, PV$^{JAK2V617F+}$ showed a significant increase of early mononuclear megakaryoblasts respect to healthy donors, associated with the parallel significant reduction of multnuclear populations. Strikingly, megakaryopoiesis morphologies of pt#1 indicated the same increase of mononuclear megakaryoblasts and a reduction of multinuclear megakaryoblasts respect to healthy donors and PV, with the complete absence of terminally differentiated populatotions (N>4), and in agreement with CD41 time curve. Surprisingly, the morphology of megakaryocytes from pt#2 presented, as pt#1, a lower number of multinuclear megakaryocytes in comparison to healthy donors and PVs, with defective production of terminal differentiated populations and the same significant increase of mononuclear megakaryoblasts (fig. 4.8, right panel).
Altogether these data suggest that pt#1 and pt#2 myelopoiesis had a major erythroid push, with a partial impairment of megakaryopoiesis, both in proliferation and differentiation.
To extensively complete the study of myeloid differentiation, we also analyzed the morphologies of CD34+ cells of pt#2 undergoing to granulopoiesis and monopoiesis (fig. 4.9). As already previously shown, HSCs from healthy donors and PVs$^{JAK2V617F+}$ were cultured as a reference of physiological and pathological myelopoiesis.

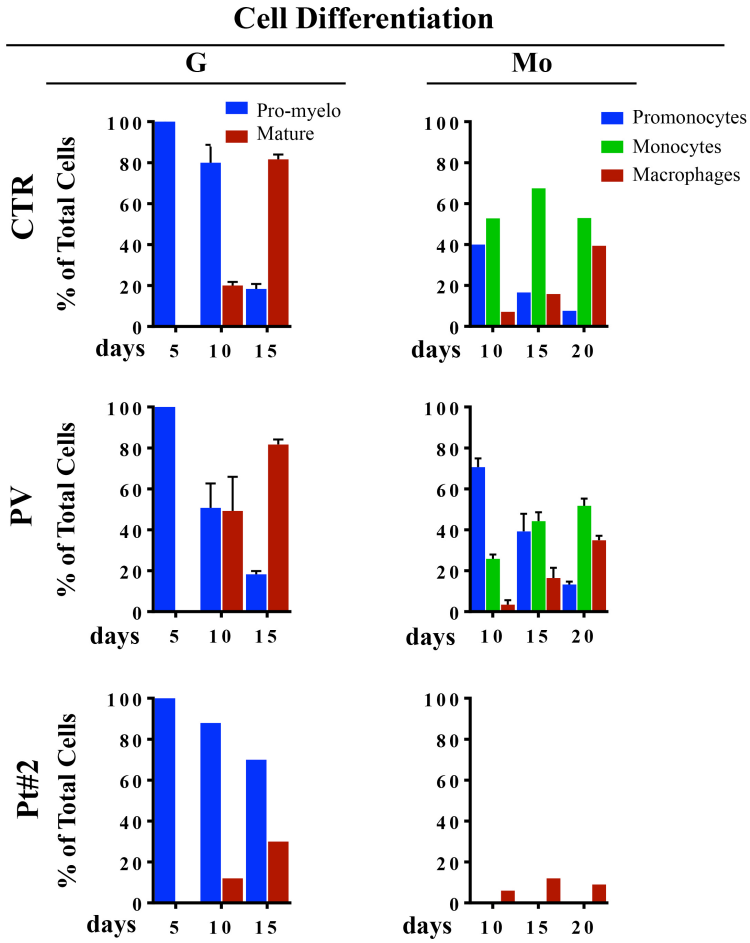

Figure 4.9. Granulocytic and monocytic differentiation of CD34+ cells from pt#2. CD34+ cells isolated from pt#2 were commited to granulocytic and monocytic differentiation under appropriate culture conditions, and relative morphologies at specific stages were assessed. For granulopoiesis, promyelocyte and mature myelocytes where distinguished and reported as percentage while for monopoiesis the differentiation morphologies of promonocytes, monocytes and macrophages have been taken in to account.

Pro-myelocite and myelocyte number did not significantly differed between controls and PV, whereas pt#2 showed a strong trend towards non-mature granulopoiesis, with an increased number of pro-myelocites (fig. 4.9, left panel). Moreover, although no major changes were observed between control and PV monocytes, an impressive absence of promonocytes and monocytes was observed for pt#2, presenting macrophages as the only differentiating population (fig. 4.9, right panel).

Taken together, these data show that pt#1 and pt#2 $CD34^{+}$ unilineage cultures have an erythroid growth propensity and megakaryopoiesis impairment, with a myelopoiesis differentiating behavior similar to $PVs^{JAK2V617F+}$, and an altered granulopoiesis and monopoiesis specifically for pt#2. Unfortunately no unilineage cultures could be conducted on pt#3.
To confirm such enhanced erythroid growth, peripheral blood progenitors from all three patients were functionally analyzed by *in vitro* colony assay. Since EPO-independent growth is a broadly known feature of polycythemia vera, we evaluated the number of BFU-E colony formation for all three patients on methylcellulose culture of peripheral blood mononuclear cells (PBMCs) at different concentrations of EPO (3, 1 and 0.1 U/ml), comparing it with the number of colony produced by healthy donors and a group of control $PV^{JAK2V617F+}$ (fig. 4.10).
Interestingly, peripheral blood progenitors of pt#1 produced a significantly higher number of BFU-E colonies than healthy donors at all growth conditions. BFU-E growth was increased as well for pt#2 and pt#3, although only at EPO 0.1 U/ml with significance, and still at lower levels than $PVs^{JAK2V617F+}$. Thus all three patients exhibited an intermediate growth trend of erythroid BFU-E colonies, with a colony number higher than healthy donor samples but inferior to our control group of $PV^{JAK2V617F+}$ (fig. 4.10.A). Conversely, CFU-GM colonies showed a significant impairment in growth for $PVs^{JAK2V617F+}$ and pts#1, 2 and 3, especially at EPO 0.1 U/ml condition (fig. 4.10.B).

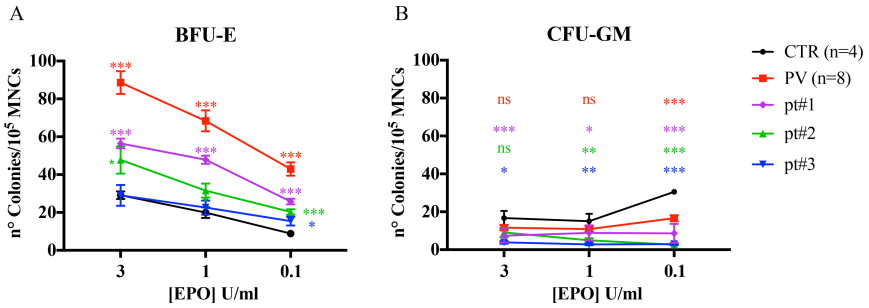

Figure 4.10. Peripheral blood progenitors of pt#1,2 and 3 form erythroid colonies on clonogenic assay. Erythroid colonies formation for healthy controls, JAK2V617F+ PVs and pt#1, pt#2 and pt#3, at EPO concentration of 3, 1 and 0,1 U/ml are shown. MNCs isolated from peripheral blood were cultured on methylcellulose and BFU-E (A) or CFU-GM (B) colonies were counted at 14 days; results are displayed as number of colonies per 10^5 MNCs. Experiments are mean of 4 healthy donor controls and 8 PV patients, whereas pt#1, pt#2 and pt#3 colonies are means of 3 independent replicates each. Statistical analysis was performed by unpaired Student's t-test, comparing each sample condition to the respective one of healthy donors controls (* = $p \leq 0,05$; ** = $p \leq 0,01$; *** = $p \leq 0,001$).

These data depict a mild PV phenotype, with an erythroid growth propensity at lower levels of erythropoietin than canonic PVs, but significantly higher than healthy individuals. Noteworthy, data from unilineage cell cultures and BFU-E colony assay complied, enforcing the hypothesis of an unbalance of myelopoiesis towards erythropoiesis for pt#1, pt#2 and pt#3, and suggesting to further investigate the importance of these CALR mutations in pathologic erythropoiesis.

4.1.4 Total CALR mRNA expression in CALR mutated MPNs positively correlates with genomic allelic burden.

We previously showed that CALR mRNA is differently expressed along myelopoiesis (fig. 4.1.A). If CALR has a lineage-dependent expression, it is reasonable that such expression might be altered in

those pathological condition such MPNs, associated to a disequilibrium of myeloid differentiation. In order to verify whether CALR expression is dependent by pathological condition of MPNs, in relation to its canonical e uncommon mutations, we measured CALR mRNA total levels in a cohort of MPNs patients, including pt#1 and pt#2, and healthy donors. No major changes in the mRNA levels were observed (data not shown). However, Pearson's r indicates that CALR allelic burden positively correlates with total mRNA expression levels, supporting the hypothesis that the amount of mutated clones is related to CALR expression (fig. 4.11).

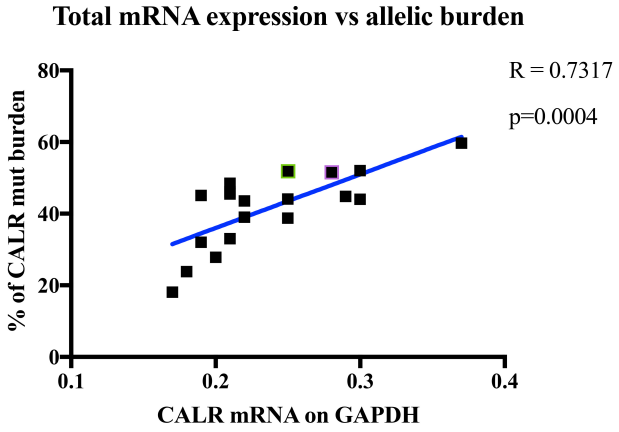

Figure 4.11. CALR mRNA levels and allelic burden measured in MPNs patients are significantly correlated according to the Pearson analysis. Data of total CALR mRNA expression from 19 CALR mutated MPNs patients, comprising pt#1 and pt#2 indicated respectively in purple and green, normalized on GAPDH were plotted in a dispersion graph and versus genomic allele burden of the same sample. Pearson'r p value = 0.0004.

4.1.5 CALR 3'UTR c.1254+10_+33del region is highly conserved among vertebrates.

Such presented data converge in outlining that CALR mutation in MPNs might have effects on the same CALR expression.

Moreover, the presence of non-canonical mutations maintaining the KDEL domain in patients clinically resembling $PV^{JAK2V617F+}$, suggest that CALR have a role in the entireness of myelopoiesis, particularly in erythropoiesis. This hypothesis is sustained by *in vitro* growth differentiation assays of primary cells bearing mutations c.1214_1225del and c.1254+10_+33del, which showed an erythroid growth push (fig 4.6-4.8). Due to our interest in functional characterization of CALR 3'UTR and intrigued by the presence of a 3'UTR deletion associated to PV, we then decided to focus on 3'UTR del24 mutation found in pts#2 and 3. Therefore, to preliminary investigate the importance of such 3'UTR region, we performed a Clustal Omega analysis on protein and RNA level, comparing the evolutionary conservation of CALR C-terminal domain with the 3'UTR region where del24 is located (fig. 4.12). Surprisingly, the nucleotides lost in del24 are part of a highly conserved 3'UTR region, with a grade of conservation that is comparable to that of protein at KDEL domain. It has to be noticed that evolutionary conservation is restricted to this region, and lost in the resting part of 3'UTR. Interestingly, this 3'UTR region comprises the trait converted in coding sequence by the +1-bp frameshift, which remove the KDEL domain, commonly observed in CALR mutated MPN. Therefore del24 determines the loss of a highly conserved 3'UTR region of CALR, potentially with functional consequences.

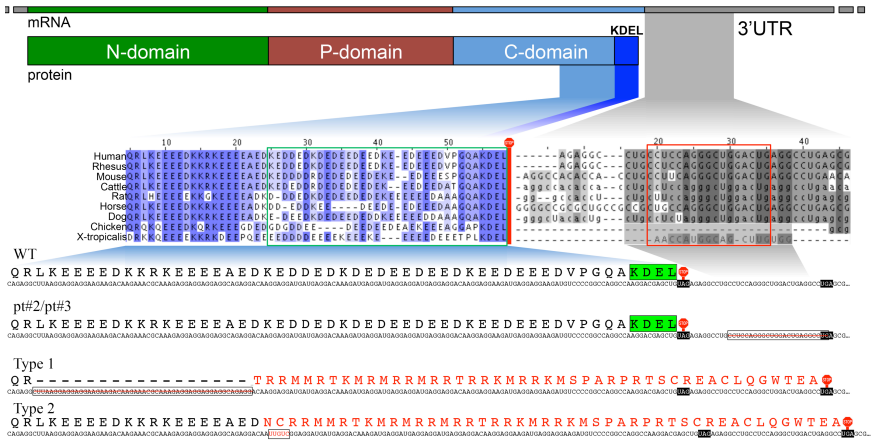

Figure 4.12. The 3'UTR region lost in del24 is evolutionarily conserved. Representation of CALR mRNA and the encoded protein (upper part); N, P, C domain with KDEL tag and 3'UTR region are indicated. Evolutionary conservation among vertebrates for protein and 3'UTR mRNA is showed in the middle section. The terminal part of protein C-domain and the early region of mRNA 3'UTR were aligned to their orthologs, showing for the human sequences the last 57 amminoacids of protein and the first 40 nucleotides of 3'UTR. Amminoacides and nucleotides conservation are respectively represented by blue and gray scale, with the darkest indicating the highest conservation. The green box highlight the protein region usually affected by common frameshift mutations observed in CALR MPNs, while the red box points out the region of nucleotides lost in del24. CALR WT and mutated variants are illustrated (bottom part), showing mRNA and the encoded protein. On mRNA, deletions and insertion are embedded within black boxes, with deletion depicted by red strikethrough, whereas insertion nucleotides are in red; on protein, novel peptides are indicated in red. KDEL domain is highlighted in green and active stop codons are illustrated by stop signs. Del 24, type 1 and type 2 mutations are compared to WT sequence.

4.1.6 CALR mutations are associated with CALR increased protein expression and activation of JAK/STAT signaling.

Recently it has been reported that several genes in a various series of tumors presented 3'UTR disruption associated with increased protein expression. To evaluate this possibility we performed a western blot analysis of PBMCs from pt#2 and pt#3, a group of CALR mutated MPNs and healthy donors. Surprisingly, CALR expression appeared augmented in CALR mutated patients and, more intriguingly, pt#2 and pt#3 showed the highest levels of the protein (fig. 4.13). In addition, we evaluated STAT5 phosphorylation levels, since JAK/STAT signaling is a primary pathway of myelopoiesis, which is aberrantly active in MPNs.

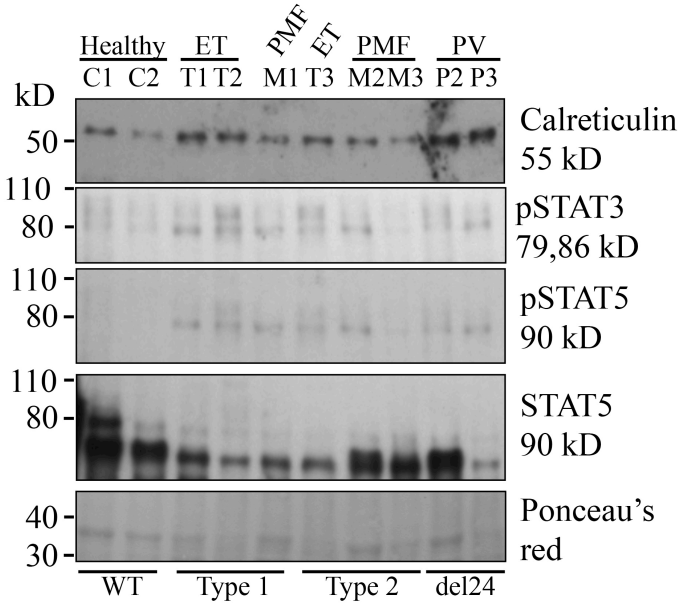

Figure 4.13. CALR expression levels are associated with MPNs and JAK-STAT pathway activation. Western-blot analysis was conducted on protein lysates from PBMCs of healthy donors controls and CALR mutated MPNs patients. Phosphorylation of STAT5 and STAT3 was measured respect to the total protein. In the upper part of panel the diagnosis is indicated, whereas

CALR mutational status is specified on the bottom part; Ponceau's red is reported as loading control.

To further investigate the asset of myelopoiesis signaling in CALR mutated patients, by western blot we analyzed JAK/STAT pathway activation in PBMCs cells from a cohort of CALR mutated MPNs, including pt#2 and pt#3. Importantly, we observed phosphorylation of STAT5 in CALR mutated MPN patients and pt#2/pt#3, and such mutations appeared to correlate with CALR expression. To further confirm these data in erythroid cells, we performed an immunofluorescence for CALR and video-confocal imaging on BFU-E isolated from pt#3 and healthy donor after 10 days of culture (fig. 4.14).

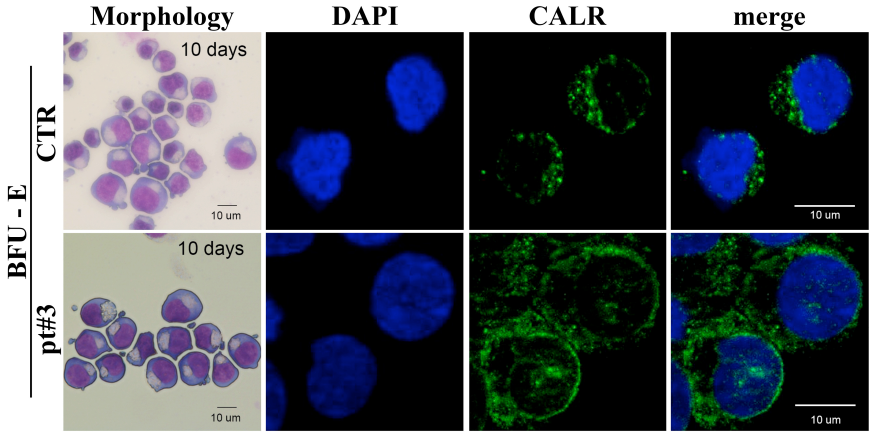

Figure 4.14. CALR del24 apparently changes the protein distribution within BFU-E erythroid progenitors. BFU-E after 10 days of culture from healthy donor and pt#3 were stained for anti-CALR, and imaged with green fluorescence. DAPI shows nuclei. A representative image of BFU-E morphology for each sample is reported. Image acquired with 60X oil immersion objective.

CALR expression in del24-BFU-E appeared increased respect to the control companion. Interestingly, the general pattern of the protein differed between the two samples. Even though the localization of CALR was mainly cytoplasmatic for both samples, in pt#3 BFU-E a slight nuclear localization was observed. Albeit it has been reported that CALR nuclear signal could be an artifact[30], such data demonstrated that 3'UTR del24 might induce anyway a different protein distribution in erythroid progenitors, regardless of effective nuclear localization.

4.2 Predictive analysis and expression of microRNAs targeting CALR at c.1254+10_+33del region.

Once studied the gene expression profiles of CALR in the context of hematopoiesis and MPNs, and considering that we detected a CALR 3'UTR deletion, the second aim of this thesis was to investigate a putative regulation network operating on CALR 3'UTR.

4.2.1 TargetScan analysis of CALR 3'UTR indicates that mir-455.3p and mir-1972 are predicted to target CALR at del24 region.

The first working hypothesis was to research miRNAs that might target CALR on the region of del24; assuming that CALR expression should be finely regulated during erythropoiesis, the lack of the specific target determined by deletion could induce the escape of CALR transcript from repression. To preliminary test such hypothesis we performed a prediction analysis by using the software TargetScanHuman (targetscan.org)[92], focusing on nucleotides 10-33 of 3'UTR. By selecting miRNAs for such specific region, we noticed that two miRNAs, possibly binding CALR 3'UTR, would have been impaired by del24. The first, mir-455.3p, is predicted to bind CALR 3'UTR at nucleotides 20-27, with a 8mer seed and a context++ score of -0,18 and is reported to target CALR in cardiac tissue of mice models[55, 56], whereas mir-1972, predicted to bind nts 28-34, has a context++ score of -0,23 and is known to induce G2-M cell cycle arrest in CML[92].

4.2.2 microRNA-455.3p is not expressed in myeloid cell lines and PBMCs of healthy donors and MPNs.

We performed real-time PCR on unilineage RNA, MPN patients, healthy donors and myeloid cell lines, detecting almost absent levels of mir-455.3p (data not showed). We performed the same test employing Digital-PCR, with more sensitivity, on the same samples, once again not detecting essentially any signal. Thus we

decided to discard the study of such miRNA, probably not expressed in the hematopoietic tissues.

4.2.3 mir1972 is expressed in myeloid cell lines and PBMCs, but CALR mRNA levels apparently are not dependent from it.
We then assayed the levels of mir1972 in MPNs patients, healthy donors and myeloid cell lines, together with CALR mRNA. Although mir-1972 was clearly detectable in granulocytes mRNA of MPNs patients, however CALR mRNA levels did not show a sharp related change in gene expression (data not shown). We are currently repeating such experiments to determine a clearer statement about mir1972-dependent CALR regulation.

4.3 An in *vitro* model for the functional characterization of *CALR* 3'UTR del24.

Afterwards the study of CALR expression in hematopoiesis and MPNs encompassing its regulation, last aim of this thesis was to investigate whether the disruption of specific regions within CALR 3'UTR might have functional implication in hematopoiesis. Since we identified a deletion of CALR 3'UTR in two PV patients, we planned to obtain an *in vitro* model of such mutation.

Hence, to study the effects of del24 in a stable cell line model, we generated CRISPR-CAS9 gene-edited K562 cells, which are a widely accepted model of erythroleukemia[93]. The choice of CRISPR-CAS9 technology relied on the chance to reproduce the deletion, acting directly on the genome of cells.

4.3.1 Reproduction of CALR 3'UTR del24 in K562 cell lines by gene editing

Upon clones screening, based on the deletion size compared with pt#2/pt#3 profile, we selected clones 20, 28 and 30 (4.15.A). By fragment analysis and Sanger sequencing, we verified that all clones successfully reported the mutation c.1254+10_+33del24, besides other partial deletions of the targeted region. Clone 20 had the mutation c.1254+13_+15del3, whereas clones 28 and 30 showed the deletion c.1254+13_+23del11; nonetheless both additional deletions are comprised within del24 region. Thus we can consider clones 20 and 28/30 as two different loss grades of del24 region. The allelic burden for clones 20, 28 and 30 was 57%, 54% and 45% respectively (fig. 4.15.B).

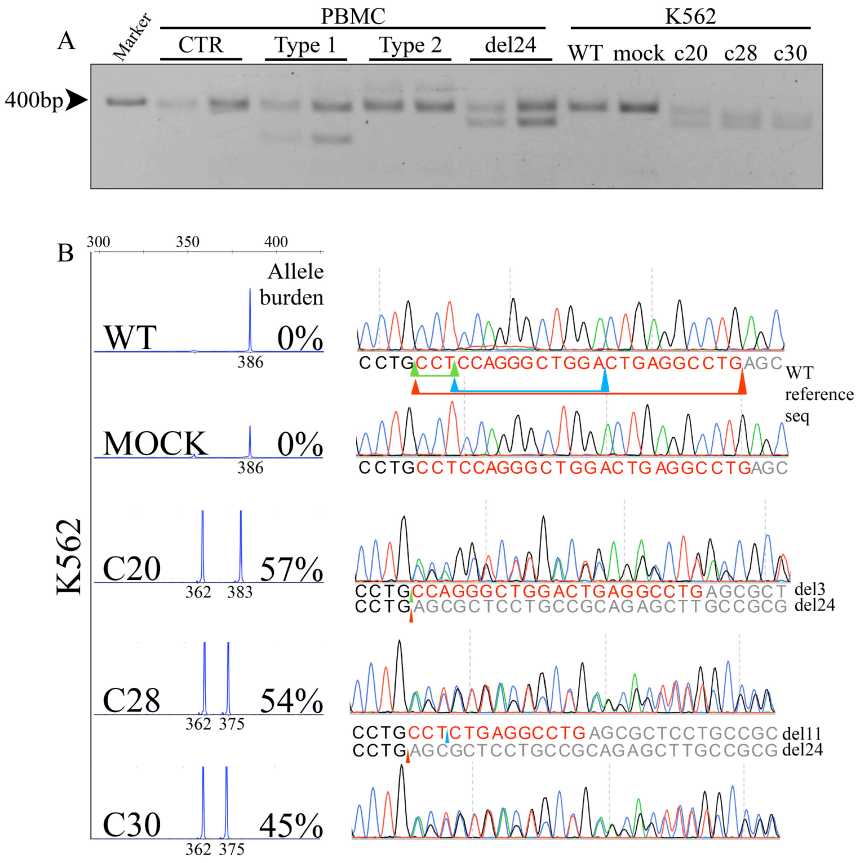

Figure 4.15. K562 successfully gene-edited to reproduce CALR del24.
(A) Genotyping assay by PCR on genomic DNA and agarose electrophoresis shows the size of mutation c.1254+10_+33del24 compared to the most recurrent CALR mutations type 1 and type 2. The same assay was performed on CRISPR-CAS-generated K562, reporting the deletions of the targeted sequence in clones 20, 28, 30. (B) Fragment analysis and Sanger sequencing of K562 genome-edited to generate CALR mutation c.1254+10_+33del24. Fragment and sequence profiles of original K562 cells, mock transduced and clones 20, 28 and 30 are shown. Nucleotide allelic size and allelic burden of each clone is reported together with mixed sequence. On wild type reference sequence red, green and blue lines-arrowheads highlight nucleotides deleted in c.1254+10_+33del24, c.1254+10_+13del3 and c.1254+13_+23del11 respectively. On clone 20,28 and 30 sequences junctions are depicted with arrowheads of the respective color.

4.3.2 CALR 3'UTR del24 is associated to increased CALR protein and activation of JAK/STAT pathway.

To assess the effect of del24 on JAK/STAT pathway within such *in vitro* model we conduced a western blot analysis that showed an increase of p-STAT5 levels for clones 20, 28 and 30 (fig. 4.16). Moreover, this finding was associated with an augmented CALR expression, supporting that the loss of del24 - nucleotides influenced the upregulation of the CALR, consistently with trends observed in vivo for pt#2 and pt#3.

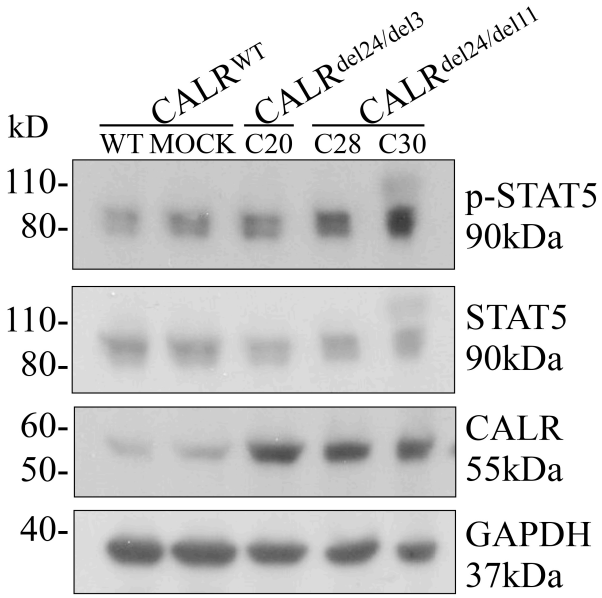

Figure 4.16. Del24 is associated with STAT5 phosphorylation and increased levels of *CALR* protein. K562 CRISPR-CAS cells bearing the mutation del24 (clone 20, 28 and 30) and original and mock transduced K562 cells were lysed and loaded on western blot for analyzing expression levels of p-STAT5 and CALR. GAPDH is shown as loading control.

4.3.3 Immunophenotype markers and cell morphologies indicate that CALR 3'UTR del24 reproduces a pro-erythroblast/erythroblast transition.

To dissect the phenotypic behavior of K562 cells following del24 gene-editing, we checked cell surface markers for stemness and myeloid lineages (fig. 4.17). Interestingly, del24 caused a decrease of CD117, from 26-27% of WT and MOCK controls to 16, 9.9 and 2.4% of clones 20, 28 and 30, which states for the assumption of a more differentiated status. Alongside we observed that the erythroid marker CD235a – glycophorin A substantially rose, from 65-70% of WT-MOCK to 81% in all gene-edited clones, while the companion marker of the same lineage CD71 resulted equally high across samples (98%). This pattern was associated with the reduction of granulocytic marker CD15 (70% of WT and MOCK versus 60% of clones 20 and 28 and 57% of clones 30).

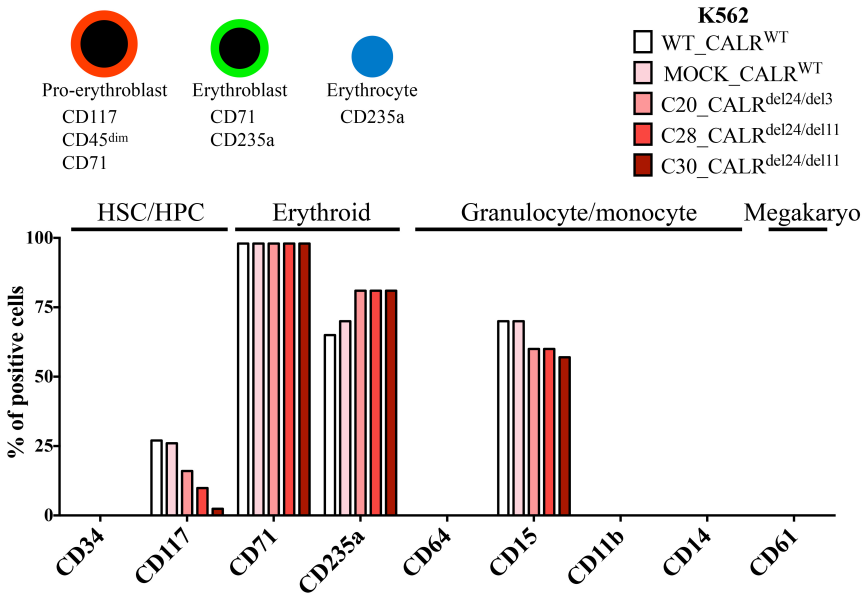

Figure 4.17. The lost of del24 nucleotides in K562 cells recapitulates the early stages of erythroid differentiation. Immunophenotype analysis of K562-CRISPR-CAS cells. HSCs (CD117), Erythroid (CD71, CD235a) and

granulocytes (CD15) markers were assessed on CRISPR-CAS cells by FACS analysis. Markers levels per each cell sample are shown as percentage referred to the total number of analyzed cells (20.000 events per each sample). CD34 (HSCs), CD64, CD11b, CD14 (granulocytes) and CD61 (megakaryocytes), despite resulted in 0% of positive events, were indicated as well. In the upper part distinctive markers of transitions stages from pro-erythroblast to erythroblast and erythrocytes are depicted. Scheme adapted from van Lochem et al., *Cytometry B Clin Cytom,, 2004*[19].

The entireness of these immunophenotypes reassumes that the loss of del24 3'UTR region caused a reduction of c-kit, alongside to an increase of CD-235a, mimicking the early differentiation steps of erythropoiesis, from pro-erythroblast to erythroblast[19]. These phenotypic changes are either compatible to the clinics of polycythemia, where a push towards erythroid differentiation is observed[94]. Notably, morphological analysis by Wrigth-Giemsa staining confirmed such data, highlighting a more basophilic cytoplasm and more condensed chromatin for del24 clones respect to WT and mock K562 controls, recalling a pro-erythroblast to erythroblast transition. Moreover some cell appeared smaller in comparison to controls (fig. 4.18.A). Such morphological changes are suggestive of a more differentiate status, clearly visible by population rearrangement from double positive CD71-CD117 cells to a population only CD71-positive, in parallel with augmented erythroid marker CD235a (4.18.B-C).

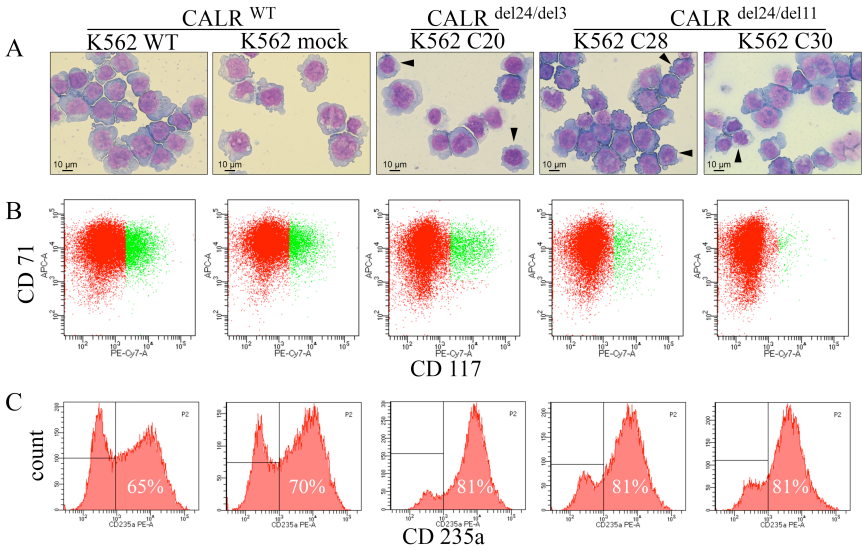

Figure 4.18. Morphologies and population analysis of gene edited K562 indicate that CALR del24 induces a differentiation event similar to transition from pro-erythroblast to erythroblast. (A) Wright-Giemsa morphology of control (WT and mock) and CRISPR-CAS (clone 20, 28 and 30) K562 cells. Per each cell line CALR genotype is indicated. Images acquired with 40X objective. Arrowheads indicate cells with erythroid differentiating morphology. B) FACS population analysis of K562 cell lines. CD117 levels are plotted versus CD71 for K562 WT, MOCK, C20, C28 and C30. Red and green indicate only CD71 positive and CD71/CD117 positive cells respectively. (C) Event count for CD235a positive and negative K562 CRISPR-CAS cells. Percentage of positive cell is indicated within the relative peak.

Taken together, these data indicate that the loss of such CALR 3'UTR region, determined by del24, induces the reprogramming of K562 cells towards erythroid differentiation, mimicking the phenotype of erythroid growth propensity observed in pt#2 and pt#3, who bear the same mutation.

4.4 RNA structural changes following genetic mutation might have implication on CALR 3'UTR function.

Recent findings propose that RNA structure is a key feature of interaction with RBPs and miRNA, and is also required for A-to-I RNA editing, particularly in the region of 3'UTR[74]. For this reason we questioned if CALR somatic mutations might affect the predicted structural folding of mRNA, generating allelic-variant derived structure.

4.4.1 pt#1 deletion c.1214_1225del, albeit located in coding sequence, is predicted to heavily alter CALR 3'UTR RNA folding.

To test such hypothesis, we analyzed the secondary structure of wild type and mutated variants of CALR mRNA by using the software Mfold (fig. 4.19). Interestingly, type 1 – del52 has a relevant impact mainly on coding sequence folding, whereas type 2 – ins5 induces very limited changes (fig. 3.19.A-C). Conversely, del24 and del12 modify mostly the 3'UTR folding. Del24, located within 3'UTR, alters the folding of coding and 3'UTR regions proximal to the deleted nucleotides (the region indicated in orange, figure D). Surprisingly del12, even if located in the coding sequence, determines dramatic structural changes of 3'UTR (cyan, orange, dark blue and brown, figure F). Thus we can hypothesize that erythroid growth phenotype observed in pt#1 might be related to functional impairment of 3'UTR, whose structure is greatly changed by del12.

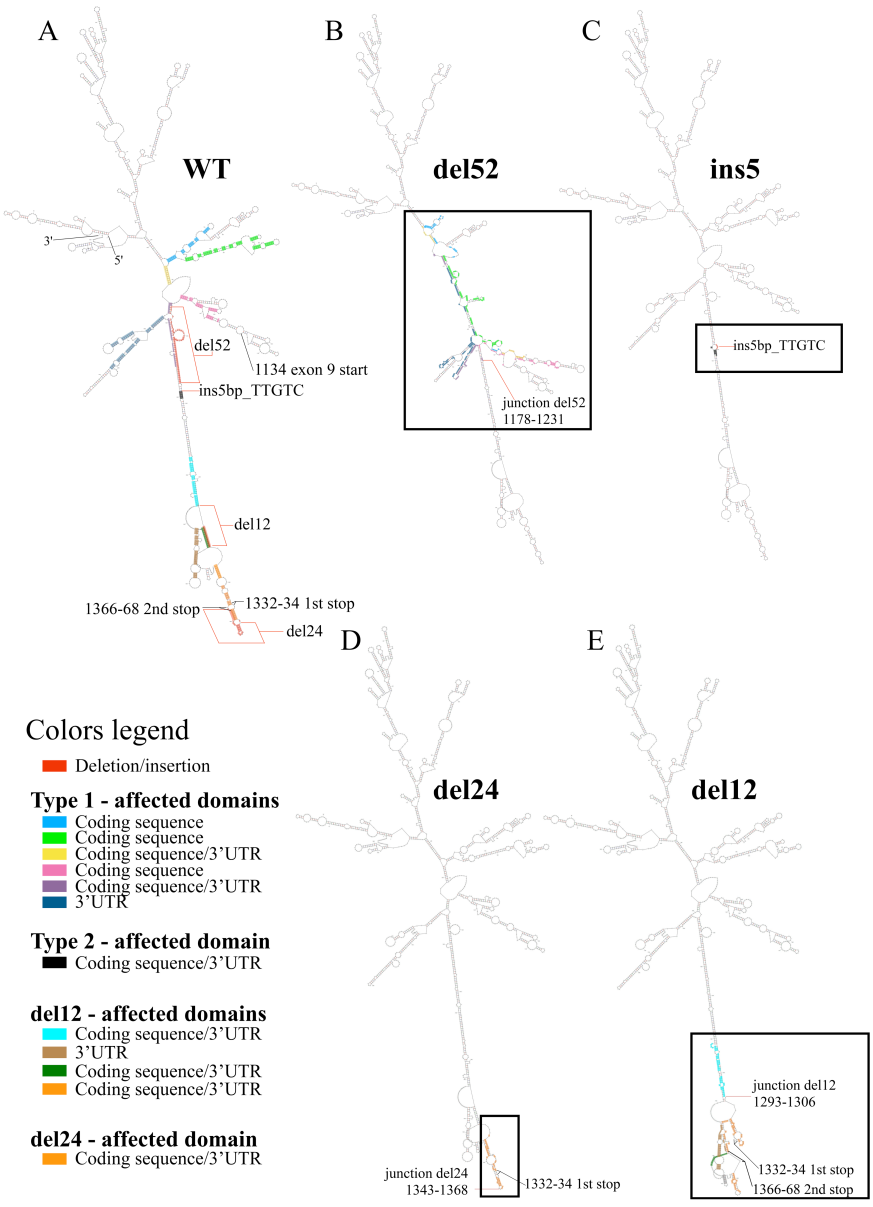

Figure 4.19. CALR mRNA structures for wild type and mutant variants. Structure prediction of folding for wild type, del52 (type 1), ins5bp (type 2), del24 and del12 mRNAs are shown. (A) Wild type CALR mRNA folding

structure is employed to map all mutations. The exon 9 start site, the 5' and 3' RNA ends and canonic stop codon, together with type1/2 stop codon are indicated. All double-strand stems of wild type structure that are affected by mutations are depicted with colors, comparing type 1 (B), type 2 (C), del12 (D) and del24 (E) with the respective wild type region. Black boxes delimit the regions affected by type1/2 and del24/de12 mutations. Secondary structures modified by type 1 mutation are shown in light blue, light green, yellow, pink, purple and dark blue. The only domain altered by type 2-mutation is indicated in black. Del24 influences the domain represented in orange. All the complex rearrangements induced by del12 affect cyan, brawn, dark-green and orange domains. Per each domain is indicated if the stem is composed by coding sequence, 3'UTR or a hybrid of both. Nucleotides lost by deletions or added by insertion are indicated in red. All nucleotides that are not affected by mutations are showed without color. RNA structure analysis was performed using the software Mfold, M. Zuker, *Nucleic Acids Res.* 31 (13), 3406-15, (2003).

5. Discussion

The present thesis aimed to investigate the role of CALR and its 3'UTR region in physiological and pathological hematopoiesis. The implications of this study are discussed below.

Here we observed a kinetic of CALR mRNA expression with high peak during physiological granulopoiesis and lower levels along megakaryocytic and erythroid differentiation. Such results appear complementary to a recent work that examined the effects of CALR overexpression and silencing in $CD34^+$ HSCs. The authors demonstrated that overexpressing CALR in HSCs by retroviral construct, leads to the increase of erythroid and megakaryocytic differentiation in both liquid and semi-solid HSCs culture. Conversely silencing CALR by short interference RNA in HSCs leads to an impaired erythropoiesis[95]. The entireness of these data indicates that a fine modulation of CALR expression might be required to ensure a proper physiological erythroid differentiation. This hypothesis is compatible with the bare expression levels of CALR mRNA that we observed in $CD34^+$ HSCs unilineage cultures (§4.1.1, fig. 4.1). The alteration of such delicate equilibrium could result in the impairment of erythropoiesis or, conversely, in its aberrant activation.

In this sense we reported the first evidence of a role of CALR 3'UTR in erythropoiesis. Indeed, we found that deletions or structural modifications of this region of CALR are associated with PV phenotypes (§4.1, fig. 4.4, §4.4, fig. 4.19). We functionally characterized the differentiating properties of progenitors cells from PV patients bearing such uncommon mutations (del12 and del24). CALR coding and 3'UTR variants del12 and del24 demonstrated an erythroid growth propensity with megakaryopoiesis impairment in $CD34^+$ unilinege cell culture, and a significant increase in BFU-E growth at low concentration of EPO, respect to healthy donors (§4.1.3, fig. 4.6-10). Moreover, CALR-del12 and CALR-3'UTR-del24 were associated with JAK/STAT signaling activation in primary PB granulocytes

isolated from pt#2/pt#3, as expected for a MPN, and more surprisingly, with the increased expression of CALR. The increase of CALR protein expression respect to healthy donors was observed either across MPNs canonical CALR mutations, albeit apparently at minor magnitudes (§4.1.4, fig. 4.11, §4.1.6, fig. 4.13).
The association between a more active status of JAK-STAT pathway and higher expression levels of CALR in PV-like pt#2 and pt#3 could be related to a work of Brusson et al. that reported the enhanced expression of CALR in $JAK2^{V617F}$ PV patients' erythrocytes[96].
These authors suggest that CALR protein, in its wild type form, can have a crucial role in erythropoiesis, as demonstrated elsewhere and previously discussed, and acts as mediator of aberrant JAK-STAT activation, which might lead to its overexpression, suggesting a JAK-STAT-dependent modulation of CALR.
It goes without saying that the genetic background of classically-defined PVs is different to our cases of pt#2 and pt#3, since JAK^{V617F} mutation is reported in 90% of PV.
Premising this, the finding of increasing CALR levels in PV is confirmed in our study despite we employed PB granulocytes, whereas Brusson et al. analyzed CALR protein levels directly on red blood cells. An intriguing hypothesis might be that CALR 3'UTR del24 or del12 perturb the same milieu signaling, where JAK/STAT pathway and CALR somehow physiologically co-operates to ensure the proper erythropoiesis, and whose alteration is more frequently observed in PV due to $JAK2^{V617F}$. Such undefined signaling network is differently perturbed by CALR 3'UTR disruption or del12 non-canonical mutation, leading to a PV-resembling phenotype, but from a different route (§4.1.3, fig 4.6-4.8, §4.1.6, fig. 4.13).
In this sense it has to be underlined that pt#1, pt#2 and pt#3 showed a mild erythroid growth of BFU-E, significantly higher than healthy donors but inferior to $JAK2^{V617F}$ PVs, indicating that

CALR 3'UTR deletion or structural alterations by non-canonical coding mutations could determine a unique subtype of polycythemia, and that JAK/STAT pathway-CALR crosstalk might occur in a bidirectional fashion.
Moreover the increase of CALR expression we observed in CALR-canonical mutated ET and PMF cases, where JAK^{V617F} mutation is absent, enforces the theory of a CALR main role in hematopoiesis, since CALR higher expression is associated anyway with the activation of JAK-STAT signaling, also in ET and PMF (§4.1.6, fig. 4.13).
Regarding the evaluation of CALR protein levels, it must be mentioned that some recent works described CALR as an intrinsically disordered protein, with an alternation of ordered and disordered domains, claiming that the protein resist to SDS, heat and even urea treatment, and setting the basis for a peculiar evaluation of its protein amounts on western blot. Indeed it is proposed that the highly dynamic structure of CALR obliges to use different antibodies directed to different epitopes, overcoming this challenging aspect[30]. Unfortunately we do not know the exact epitope of the employed anti-CALR antibody. Nevertheless, we can reasonably hypothesize that whatever domain of CALR we observed, the data are still valid for that domain, or can be a measure of how accessible such domain is, possibly indicating that CALR change its conformation as consequence of its mutations.
Differently from del12, already reported in PMF, to our knowledge CALR 3'UTR del24 (c.1254+10_+33del24) is described here for the first time, in MPNs. We cannot rule out that del24 is a rare genetic event, not routinely recognizable in daily diagnostic of MPNs; anyway, these uncommon alterations unveiled a hide side of CALR functions in *in vivo* myelopoiesis. Moreover, it should be considered that the majority of NGS sequencing on MPNs focuses only on coding sequence[82, 97, 98]. Therefore systematical screening of CALR 3'UTR, at least in those cases of erythrocytosis not presenting any mutations included in WHO criteria, can reveal a

novel aspect of PV etiology, and may clarify if our case is a rare finding or a recurrent genotype ignored so far.
Regrettably, we did not obtain an *in vitro* model of del12 on time for this study. We are currently work to generate cell lines overexpressing del12-CALR by lentiviral construct, as well as CRISPR-CAS9 model of such deletion. Nevertheless we propose that the heavy modification of 3'UTR RNA structure that del12 is predicted to determine might explain the effects of such mutation on erythroid growth, with a mechanism still to be identified (§4.4, fig. 4.19). Certainly, del12 determines the in-frame deletion of 4 aa within CALR C-domain, which has been found involved in several CALR functions, whose the most extensively studied is Ca^{++} binding. Beside 3'UTR RNA structural alterations, the study of possible modifications on Ca^{++} binding properties could clarify the effects of del12 on erythropoiesis, even in light of the fact that Ca^{++} is implied in EPOR signaling[99-101].
Conversely, for CALR 3'UTR-del24 we had the opportunity to study the effect of such deletion *in vitro.* Our K562 CRISPR-CAS9 model confirmed the trend of an increased CALR expression and a more active JAK/STAT pathway complied with del24 (§4.3.2, fig. 4.16). Importantly the deletion resulted either in morphological and immunophenotypic modifications that are similar to the early stages of erythroid differentiation (§4.3.3, fig. 4.17). This is in accordance with Polycythemia Vera, where a faster maturation in erythropoiesis is observed exactly at those early stages[102].
The evolutionary conservation among vertebrates of the region comprised within the first 30-40 bases of CALR 3'UTR, where del24 is located, was previously reported for mammals[57], and is indicative of a potential functional importance of such region (§4.1.5, fig. 4.12). Moreover the fact that part of this region is converted in coding sequence by canonical CALR mutations is an aspect that could deserve further investigations. Furthermore, we detected such mutation in saliva cells, suggesting a genetic inheritance of the genetic lesion (§4.1.2, fig. 4.5). Several hereditary coding mutations are known to naturally favor the onset

of tumors. However the finding that a 3'UTR alteration hereditarily transferred predisposes to a pre-tumoral condition is an unexpected implication for a non-coding mutation, which might have functional consequences even on other tissues beyond the hematopoietic lineages.
If a 3'UTR deletion could determine phenotypic effects within a pathological context, we can hypothesize that those effects are linked to some mRNA functions. Recently several functional roles of 3'UTR have been reported, related to RNA-dependent protein localization, translation efficiency and miRNA escape. Regarding microRNA-regulated gene expression, the first hypothesis suggested that when a crucial regulative element of 3'UTR is lost, due to the formation of a shortened 3'UTR by alternative polyadenilation or as result of a genetic deletion, such the case of c.1254+10_+33del24, those transcripts "escape" from mi-RNA repression, leading to their overexpression as oncogenes and cancer[65, 72]. Then further works proposed that the same alterations could affect either tumor suppressor genes, since the lost 3'UTR traits might also result in a simple positional change of miRNA target sites, which improve their repression efficiency[68]. Furthermore, ceRNAs have been recently described to free up microRNAs, physiologically sequestered, as consequence of 3'UTR shortening, causing tumor suppression repression as well[103]. To investigate the hypothesis of CALR miRNA escape induced by del24, we tested both mir-455.3p and mir-1972 as putative regulator of CALR targeting the region lost in del24. However, we observed no expression of miR-455.3p, both in cell lines and primary cells (data not shown), whereas data about miR-1972 need further investigations (§4.2.1-3). Thus we are currently studying the aspect of miRNA regulation of CALR and a possible implication of del24 in miRNA-escape. Beyond the aims of this study, an extensive analysis of miRNA data set expression in MPNs, by selecting those miRNAs down-regulated in JAK^{V617F}-PV, and then filtering them based on a seed sequence which have to be complementary to CALR del24, might more efficiently

identify miRNAs as candidate-regulators of CALR. Moreover, we also evaluated the implications of del12 and del24 on CALR mRNA structure, reporting that del24 and, more dramatically, del12 heavly affect RNA folding of 3'UTR region. (§4.4.1, fig. 4.19) In this sense either miRNA targeting analysis might be extended to the regions flanking the deletion, selecting sequence traits according the criterion of RNA folding alteration. Indeed all putative miRNAs potentially binding the regions surrounding the mutations could result impaired in their function by such heavy structural changes of RNA.
Said that, if a miRNA would be implied in this effect we observed in PV, CALR del24 might have a finer impact on HSC homeostasis than those observed for overexpression and repression of proto-oncogenes and tumor suppressor respectively, since in PV there is a proliferative trend of the erythroid lineage, but anyway with a complete and physiological differentiation. Indeed an effect of CALR expression levels on erythropoiesis and myelopoiesis in general has been already described, as previously discussed, and confirmed in this study. Moreover CALR evidences as a proto-oncogene are yet contrasting[52], probably for the reason of its multiple functions. Thus we can hypothesize that the fine regulation of CALR expression might act crucially on erythroid differentiation, and even a minimal upregulation could push more myeloid progenitors to the erythroid lineage. This is compatible with the proliferative but benign condition of PV that is a pre-tumoral stage, differently from heavier changes required for the onset of cancer.
Moreover, 3'UTR have been observed regulating protein localization, acting as a protein-interaction scaffold[63]. Our data on CALR localization encourages further studies of this hypothesis, since we observed a partially nuclear localization (§4.1.6, fig. 4.14). Recent literature refuses this theory, as apparent CALR nuclear localization seems to be a misleading artifact, due to CALR role in GR nuclear importing/exporting, that bring the protein at the perinuclear boundary of ER, close to the nucleus but

outside it[39]. Even though our technique should visualize a single confocal plane of BFU-E, thus a inner section respect to the nucleus, further experiments could clarify this aspect, reaching new insights also on 3'UTR-dependent protein localization.
Beyond all mechanisms involving RNA-related 3'UTR functions, it deserves to be mentioned a parallel hypothesis contemplating that 3'UTR sequence traits act as recruiting elements for transcription factors directly on DNA. This might lead to the engagement of chromatin remodeling complexes, causing the spread of specific histone modifications. Moreover, as widely known, enhancers might regulate gene expression even at several kb of distance from target gene[104, 105]. Such additional degree of complexity further extends the functional potential of 3'UTR sequences, and the consequences that their lost might determine.
An exciting and actually uncovered field regards the study of any possible mechanism regulating CALR expression and function by acting on its 3'UTR sequence, thus understanding how the alteration of CALR 3'UTR might affect erythropoiesis and PV onset within the context of MPNs. Novel findings on this mechanisms could ameliorate an early diagnosis, prognosis and possibly therapy of MPN, besides to clarifying fine regulation operating behind erythropoiesis.

REFERENCES

1. S.H. Orkin *et al.*, Hematopoiesis: An Evolving Paradigm for Stem Cell Biology. *Cell*, 2008. 132(4): p. 631-44.

2. E. Dzierzak *et al.*, Erythropoiesis: Development and Differentiation. *Cold Spring Harb Perspect Med*, 2013. 3(4): p. a011601.

3. M.W. Long *et al.*, Phorbol Diesters Stimulate the Development of an Early Murine Progenitor Cell. The Burst-Forming Unit-Megakaryocyte. *J Clin Invest*, 1985. 76(2): p. 431-8.

4. Y. Iizuka *et al.*, A Quantitative Assay for Mouse Granulocyte (Cfu-G) and Macrophage (Cfu-M) Precursors Using Plasma Clots. *J Histochem Cytochem*, 1985. 33(7): p. 617-23.

5. N.N. Iscove *et al.*, Erythroid Progenitors in Mouse Bone Marrow Detected by Macroscopic Colony Formation in Culture. *Exp Hematol*, 1975. 3(1): p. 32-43.

6. E. Laurenti *et al.*, From Haematopoietic Stem Cells to Complex Differentiation Landscapes. *Nature*, 2018. 553(7689): p. 418-426.

7. J. Adolfsson *et al.*, Upregulation of Flt3 Expression within the Bone Marrow Lin(-)Sca1(+)C-Kit(+) Stem Cell Compartment Is Accompanied by Loss of Self-Renewal Capacity. *Immunity*, 2001. 15(4): p. 659-69.

8. J.L. Christensen *et al.*, Flk-2 Is a Marker in Hematopoietic Stem Cell Differentiation: A Simple Method to Isolate Long-Term Stem Cells. *Proc Natl Acad Sci U S A*, 2001. 98(25): p. 14541-6.

9. A. Wilson *et al.*, Hematopoietic Stem Cells Reversibly Switch from Dormancy to Self-Renewal During Homeostasis and Repair. *Cell*, 2008. 135(6): p. 1118-29.

10. H. Oguro *et al.*, Slam Family Markers Resolve Functionally Distinct Subpopulations of Hematopoietic Stem Cells and Multipotent Progenitors. *Cell Stem Cell*, 2013. 13(1): p. 102-16.

11. E.M. Pietras *et al.*, Functionally Distinct Subsets of Lineage-Biased Multipotent Progenitors Control Blood Production in Normal and Regenerative Conditions. *Cell Stem Cell*, 2015. 17(1): p. 35-46.

12. K. Akashi *et al.*, A Clonogenic Common Myeloid Progenitor That Gives Rise to All Myeloid Lineages. *Nature*, 2000. 404(6774): p. 193-7.

13. M. Kondo *et al.*, Identification of Clonogenic Common Lymphoid Progenitors in Mouse Bone Marrow. *Cell*, 1997. 91(5): p. 661-72.

14. J.R. Stephenson *et al.*, Induction of Colonies of Hemoglobin-Synthesizing Cells by Erythropoietin in Vitro. *Proc Natl Acad Sci U S A*, 1971. 68(7): p. 1542-6.

15. C.J. Gregory *et al.*, Human Marrow Cells Capable of Erythropoietic Differentiation in Vitro: Definition of Three Erythroid Colony Responses. *Blood*, 1977. 49(6): p. 855-64.

16. C.J. Gregory *et al.*, Erythropoietic Progenitors Capable of Colony Formation in Culture: State of Differentiation. *J Cell Physiol*, 1973. 81(3): p. 411-20.

17. J. Li *et al.*, Isolation and Transcriptome Analyses of Human Erythroid Progenitors: Bfu-E and Cfu-E. *Blood*, 2014. 124(24): p. 3636-45.

18. D.S. Krause *et al.*, Right on Target: Eradicating Leukemic Stem Cells. *Trends Mol Med*, 2007. 13(11): p. 470-81.

19. E.G. van Lochem *et al.*, Immunophenotypic Differentiation Patterns of Normal Hematopoiesis in Human Bone Marrow: Reference Patterns for Age-Related Changes and Disease-Induced Shifts. *Cytometry B Clin Cytom*, 2004. 60(1): p. 1-13.

20. E. Bousoik *et al.*, "Do We Know Jack" About Jak? A Closer Look at Jak/Stat Signaling Pathway. *Front Oncol*, 2018. 8: p. 287.

21. F. Rosenbauer *et al.*, Transcription Factors in Myeloid Development: Balancing Differentiation with Transformation. *Nat Rev Immunol*, 2007. 7(2): p. 105-17.

22. J.L. Spivak, Myeloproliferative Neoplasms. *N Engl J Med*, 2017. 376(22): p. 2168-2181.

23. M. Michalak *et al.*, CALR, a Multi-Process Calcium-Buffering Chaperone of the Endoplasmic Reticulum. *Biochem J*, 2009. 417(3): p. 651-66.

24. D.B. Williams, Beyond Lectins: The Calnexin/CALR Chaperone System of the Endoplasmic Reticulum. *J Cell Sci*, 2006. 119(Pt 4): p. 615-23.

25. C. Bastianutto *et al.*, Overexpression of CALR Increases the Ca2+ Capacity of Rapidly Exchanging Ca2+ Stores and Reveals Aspects of Their Lumenal Microenvironment and Function. *J Cell Biol*, 1995. 130(4): p. 847-55.

26. J. Lynch *et al.*, CALR Signals Upstream of Calcineurin and Mef2c in a Critical Ca(2+)-Dependent Signaling Cascade. *J Cell Biol*, 2005. 170(1): p. 37-47.

27. I.L. Conte *et al.*, The Interplay between Calcium and the in Vitro Lectin and Chaperone Activities of CALR. *Biochemistry*, 2007. 46(15): p. 4671-80.

28. S.G. Boelt *et al.*, Mapping the Ca(2+) Induced Structural Change in CALR. *J Proteomics*, 2016. 142: p. 138-48.

29. B.A. Miller *et al.*, Erythropoietin Stimulates a Rise in Intracellular-Free Calcium Concentration in Single Bfu-E Derived Erythroblasts at Specific Stages of Differentiation. *Blood*, 1989. 73(5): p. 1188-94.

30. L. Varricchio *et al.*, CALR: Challenges Posed by the Intrinsically Disordered Nature of CALR to the Study of Its Function. *Front Cell Dev Biol*, 2017. 5: p. 96.

31. S.J. Gardai *et al.*, Cell-Surface CALR Initiates Clearance of Viable or Apoptotic Cells through Trans-Activation of Lrp on the Phagocyte. *Cell*, 2005. 123(2): p. 321-34.

32. S.J. Wijeyesakere *et al.*, The C-Terminal Acidic Region of CALR Mediates Phosphatidylserine Binding and Apoptotic Cell Phagocytosis. *J Immunol*, 2016. 196(9): p. 3896-3909.

33. M.V. Rojiani *et al.*, In Vitro Interaction of a Polypeptide Homologous to Human Ro/Ss-a Antigen (CALR) with a Highly Conserved Amino Acid Sequence in the Cytoplasmic Domain of Integrin Alpha Subunits. *Biochemistry*, 1991. 30(41): p. 9859-66.

34. M.G. Coppolino *et al.*, Ligand-Specific, Transient Interaction between Integrins and CALR During Cell Adhesion to Extracellular Matrix Proteins Is Dependent Upon Phosphorylation/Dephosphorylation Events. *Biochem J*, 1999. 340 (Pt 1): p. 41-50.

35. S. Dedhar *et al.*, Inhibition of Nuclear Hormone Receptor Activity by CALR. *Nature*, 1994. 367(6462): p. 480-3.

36. M. Opas *et al.*, Regulation of Expression and Intracellular Distribution of CALR, a Major Calcium Binding Protein of Nonmuscle Cells. *J Cell Physiol*, 1991. 149(1): p. 160-71.

37. M. Michalak *et al.*, Endoplasmic Reticulum Form of CALR Modulates Glucocorticoid-Sensitive Gene Expression. *J Biol Chem*, 1996. 271(46): p. 29436-45.

38. J.M. Holaska *et al.*, Ca2+-Dependent Nuclear Export Mediated by CALR. *Mol Cell Biol*, 2002. 22(17): p. 6286-97.

39. M. Falchi *et al.*, The CALR Control of Human Stress Erythropoiesis Is Impaired by Jak2v617f in Polycythemia Vera. *Exp Hematol*, 2017. 50: p. 53-76.

40. N.K. Singh *et al.*, Identification of CALR as a Rubella Virus Rna Binding Protein. *Proc Natl Acad Sci U S A*, 1994. 91(26): p. 12770-4.

41. L.T. Timchenko *et al.*, CALR Interacts with C/Ebp and C/Ebp Mrnas and Represses Translation of C/Ebp Proteins. *Molecular and Cellular Biology*, 2002. 22(20): p. 7242-7257.

42. P. Iakova *et al.*, Competition of Cugbp1 and CALR for the Regulation of P21 Translation Determines Cell Fate. *Embo j*, 2004. 23(2): p. 406-17.

43. D. Helbling *et al.*, The Leukemic Fusion Gene Aml1-Mds1-Evi1 Suppresses Cebpa in Acute Myeloid Leukemia by Activation of CALR. *Proc Natl Acad Sci U S A*, 2004. 101(36): p. 13312-7.

44. J.A. Schardt *et al.*, Unfolded Protein Response Suppresses Cebpa by Induction of CALR in Acute Myeloid Leukaemia. *J Cell Mol Med*, 2010. 14(6b): p. 1509-19.

45. N. Afshar *et al.*, Retrotranslocation of the Chaperone CALR from the Endoplasmic Reticulum Lumen to the Cytosol. *Mol Cell Biol*, 2005. 25(20): p. 8844-53.

46. C. Marty *et al.*, CALR Mutants in Mice Induce an Mpl-Dependent Thrombocytosis with Frequent Progression to Myelofibrosis. *Blood*, 2016. 127(10): p. 1317-24.

47. I. Chachoua *et al.*, Thrombopoietin Receptor Activation by Myeloproliferative Neoplasm Associated CALR Mutants. *Blood*, 2016. 127(10): p. 1325-35.

48. M. Araki *et al.*, Activation of the Thrombopoietin Receptor by Mutant CALR in Calr-Mutant Myeloproliferative Neoplasms. *Blood*, 2016. 127(10): p. 1307-16.

49. D. Pietra *et al.*, Differential Clinical Effects of Different Mutation Subtypes in Calr-Mutant Myeloproliferative Neoplasms. *Leukemia*, 2016. 30(2): p. 431-8.

50. G. Stoll *et al.*, CALR Expression: Interaction with the Immune Infiltrate and Impact on Survival in Patients with Ovarian and Non-Small Cell Lung Cancer. *Oncoimmunology*, 2016. 5(7): p. e1177692.

51. E. Cruz-Ramos *et al.*, Differential Expression and Molecular Interactions of Chromosome Region Maintenance 1 and CALR Exportins in Breast Cancer Cells. *J Steroid Biochem Mol Biol*, 2018.

52. M. Zamanian *et al.*, CALR and Cancer. *Pathol Oncol Res*, 2013. 19(2): p. 149-54.

53. L. Guo *et al.*, Coup-Tf1 Antagonizes Nkx2.5-Mediated Activation of the CALR Gene During Cardiac Development. *J Biol Chem*, 2001. 276(4): p. 2797-801.

54. Y. Qiu *et al.*, Regulation of the CALR Gene by Gata6 and Evi-1 Transcription Factors. *Biochemistry*, 2008. 47(12): p. 3697-704.

55. C. Wu *et al.*, Effects of Mirna-455 on Cardiac Hypertrophy Induced by Pressure Overload. *Int J Mol Med*, 2015. 35(4): p. 893-900.

56. P.J. Belmont *et al.*, Regulation of Microrna Expression in the Heart by the Atf6 Branch of the Er Stress Response. *J Mol Cell Cardiol*, 2012. 52(5): p. 1176-82.

57. D. Vuppalanchi *et al.*, Conserved 3'-Untranslated Region Sequences Direct Subcellular Localization of Chaperone Protein Mrnas in Neurons. *J Biol Chem*, 2010. 285(23): p. 18025-38.

58. P. Connerty *et al.*, Rna Binding Proteins in the Mirna Pathway. *Int J Mol Sci*, 2015. 17(1).

59. C. Mayr, Evolution and Biological Roles of Alternative 3'utrs. *Trends Cell Biol*, 2016. 26(3): p. 227-237.

60. J.J. An *et al.*, Distinct Role of Long 3' Utr Bdnf Mrna in Spine Morphology and Synaptic Plasticity in Hippocampal Neurons. *Cell*, 2008. 134(1): p. 175-87.

61. J.M. Taliaferro *et al.*, Distal Alternative Last Exons Localize Mrnas to Neural Projections. *Mol Cell*, 2016. 61(6): p. 821-33.

62. P.A. Pinto *et al.*, Rna Polymerase Ii Kinetics in Polo Polyadenylation Signal Selection. *Embo j*, 2011. 30(12): p. 2431-44.

63. B.D. Berkovits *et al.*, Alternative 3' Utrs Act as Scaffolds to Regulate Membrane Protein Localization. *Nature*, 2015. 522(7556): p. 363-7.

64. M.P. Chao *et al.*, Therapeutic Antibody Targeting of Cd47 Eliminates Human Acute Lymphoblastic Leukemia. *Cancer Res*, 2011. 71(4): p. 1374-84.

65. C. Mayr *et al.*, Widespread Shortening of 3'utrs by Alternative Cleavage and Polyadenylation Activates Oncogenes in Cancer Cells. *Cell*, 2009. 138(4): p. 673-84.

66. M. Chen *et al.*, 3' Utr Lengthening as a Novel Mechanism in Regulating Cellular Senescence. *Genome Res*, 2018.

67. A. Grimson *et al.*, Microrna Targeting Specificity in Mammals: Determinants Beyond Seed Pairing. *Mol Cell*, 2007. 27(1): p. 91-105.

68. J.W. Nam *et al.*, Global Analyses of the Effect of Different Cellular Contexts on Microrna Targeting. *Mol Cell*, 2014. 53(6): p. 1031-1043.

69. Y. Hoffman *et al.*, 3'utr Shortening Potentiates Microrna-Based Repression of Pro-Differentiation Genes in Proliferating Human Cells. *PLoS Genet*, 2016. 12(2): p. e1005879.

70. S. Diederichs *et al.*, The Dark Matter of the Cancer Genome: Aberrations in Regulatory Elements, Untranslated Regions, Splice Sites, Non-Coding Rna and Synonymous Mutations. *EMBO Mol Med*, 2016. 8(5): p. 442-57.

71. H.H. Woo *et al.*, Phenotype of Vigilin Expressing Breast Cancer Cells Binding to the 69 Nt 3'utr Element in Csf-1r Mrna. *Transl Oncol*, 2018. 12(1): p. 106-115.

72. K. Kataoka *et al.*, Aberrant Pd-L1 Expression through 3'-Utr Disruption in Multiple Cancers. *Nature*, 2016. 534(7607): p. 402-6.

73. J. Slotta-Huspenina *et al.*, The Impact of Cyclin D1 Mrna Isoforms, Morphology and P53 in Mantle Cell Lymphoma: P53 Alterations and Blastoid Morphology Are Strong Predictors of a High Proliferation Index. *Haematologica*, 2012. 97(9): p. 1422-30.

74. M.A. Zipeto *et al.*, Rna Rewriting, Recoding, and Rewiring in Human Disease. *Trends Mol Med*, 2015. 21(9): p. 549-59.

75. M.A. Zipeto *et al.*, Adar1 Activation Drives Leukemia Stem Cell Self-Renewal by Impairing Let-7 Biogenesis. *Cell Stem Cell*, 2016. 19(2): p. 177-191.

76. Q. Wang *et al.*, Requirement of the Rna Editing Deaminase Adar1 Gene for Embryonic Erythropoiesis. *Science*, 2000. 290(5497): p. 1765-8.

77. C.J. Lewis *et al.*, Rna Modifications and Structures Cooperate to Guide Rna-Protein Interactions. *Nat Rev Mol Cell Biol*, 2017. 18(3): p. 202-210.

78. J. Grinfeld *et al.*, Classification and Personalized Prognosis in Myeloproliferative Neoplasms. *N Engl J Med*, 2018. 379(15): p. 1416-1430.

79. C. Mayr, Regulation by 3'-Untranslated Regions. *Annu Rev Genet*, 2017. 51: p. 171-194.

80. J. Li *et al.*, The Emerging Roles of 3' Untranslated Regions in Cancer. *Cancer Lett*, 2013. 337(1): p. 22-5.

81. S.A. Miller *et al.*, A Simple Salting out Procedure for Extracting DNA from Human Nucleated Cells. *Nucleic Acids Res*, 1988. 16(3): p. 1215.

82. J. Nangalia *et al.*, Somatic Calr Mutations in Myeloproliferative Neoplasms with Nonmutated Jak2. *N Engl J Med*, 2013. 369(25): p. 2391-2405.

83. S. Jeromin *et al.*, Next-Generation Deep-Sequencing Detects Multiple Clones of Calr Mutations in Patients with Bcr-Abl1 Negative Mpn. *Leukemia*, 2016. 30(4): p. 973-6.

84. O.H. Lowry *et al.*, Protein Measurement with the Folin Phenol Reagent. *J Biol Chem*, 1951. 193(1): p. 265-75.

85. N.E. Sanjana *et al.*, Improved Vectors and Genome-Wide Libraries for Crispr Screening. *Nat Methods*, 2014. 11(8): p. 783-784.

86. O. Shalem *et al.*, Genome-Scale Crispr-Cas9 Knockout Screening in Human Cells. *Science*, 2014. 343(6166): p. 84-87.

87. F.A. Ran *et al.*, Double Nicking by Rna-Guided Crispr Cas9 for Enhanced Genome Editing Specificity. *Cell*, 2013. 154(6): p. 1380-9.

88. L. Vian *et al.*, Transcriptional Fine-Tuning of Microrna-223 Levels Directs Lineage Choice of Human Hematopoietic Progenitors. *Cell Death Differ*, 2014. 21(2): p. 290-301.

89. A. Tefferi *et al.*, The Prognostic Advantage of CALR Mutations in Myelofibrosis Might Be Confined to Type 1 or Type 1-Like Calr Variants. *Blood*, 2014. 124(15): p. 2465-6.

90. N. Szuber *et al.*, Novel Germline Mutations in the CALR Gene: Implications for the Diagnosis of Myeloproliferative Neoplasms. *J Clin Pathol*, 2016.

91. M. Rashid *et al.*, Coexisting Jak2v617f and Calr Exon 9 Mutation in Essential Thrombocythemia. *Indian J Hematol Blood Transfus*, 2016. 32(Suppl 1): p. 112-116.

92. V. Agarwal *et al.*, Predicting Effective Microrna Target Sites in Mammalian Mrnas. *Elife*, 2015. 4.

93. A. Finotti *et al.*, Development and Characterization of K562 Cell Clones Expressing Bcl11a-Xl: Decreased Hemoglobin Production with Fetal Hemoglobin Inducers and Its Rescue with Mithramycin. *Exp Hematol*, 2015. 43(12): p. 1062-1071.e3.

94. A. Tefferi *et al.*, Polycythemia Vera: Scientific Advances and Current Practice. *Semin Hematol*, 2005. 42(4): p. 206-20.

95. S. Salati *et al.*, CALR Affects Hematopoietic Stem/Progenitor Cell Fate by Impacting Erythroid and Megakaryocytic Differentiation. *Stem Cells Dev*, 2017.

96. M. Brusson *et al.*, Enhanced CALR Expression in Red Cells of Polycythemia Vera Patients Harboring the Jak2v617f Mutation. *Haematologica*, 2017. 102(7): p. e241-e244.

97. J.D. Milosevic Feenstra *et al.*, Whole-Exome Sequencing Identifies Novel Mpl and Jak2 Mutations in Triple-Negative Myeloproliferative Neoplasms. *Blood*, 2016. 127(3): p. 325-32.

98. E. Tenedini *et al.*, Targeted Cancer Exome Sequencing Reveals Recurrent Mutations in Myeloproliferative Neoplasms. *Leukemia*, 2014. 28(5): p. 1052-9.

99. J. Misiti *et al.*, Erythropoiesis in Vitro. Role of Calcium. *J Clin Invest*, 1979. 64(6): p. 1573-9.

100. N. Divecha *et al.*, Phospholipid Signaling. *Cell*, 1995. 80(2): p. 269-78.

101. I. Hirschler-Laszkiewicz *et al.*, Trpc2 Depletion Protects Red Blood Cells from Oxidative Stress-Induced Hemolysis. *Exp Hematol*, 2012. 40(1): p. 71-83.

102. H. Bruchova *et al.*, Erythropoiesis in Polycythemia Vera Is Hyper-Proliferative and Has Accelerated Maturation. *Blood Cells Mol Dis*, 2009. 43(1): p. 81-7.

103. H.J. Park *et al.*, 3' Utr Shortening Represses Tumor-Suppressor Genes in Trans by Disrupting Cerna Crosstalk. *Nat Genet*, 2018. 50(6): p. 783-789.

104. H. Szutorisz *et al.*, Formation of an Active Tissue-Specific Chromatin Domain Initiated by Epigenetic Marking at the Embryonic Stem Cell Stage. *Mol Cell Biol*, 2005. 25(5): p. 1804-20.

105. A.G. West *et al.*, Remote Control of Gene Transcription. *Hum Mol Genet*, 2005. 14 Spec No 1: p. R101-11.